Fall 2017

Quantification and Characterization of Net Precipitation Bacterial Flux From a Subtropical Epiphyte-Laden Oak Forest

Preston Pound

QUANTIFICATION AND CHARACTERIZATION OF NET PRECIPITATION BACTERIAL FLUX FROM A SUBTROPICAL EPIPHYTE-LADEN OAK FOREST

by

PRESTON THOMAS POUND

(Under the Direction of John Van Stan)

ABSTRACT

Transport pathways of microbes between ecosystem spheres (atmosphere, phyllosphere, and pedosphere) represent major fluxes in nutrient cycles and have the potential to significantly affect microbially-mediated biogeochemical processes. We quantified a previously unexamined microbial flux from the phyllosphere to the pedosphere during rainfall via throughfall (rainfall dripping from the canopy and through gaps) and stemflow (rainwater funneled down the stem) using flow cytometry and validated with quantitative Polymerase Chain Reaction (qPCR) assays for samples from a *Quercus virginiana* (oak) forest with heavy epiphyte cover (*Tillandsia usneoides*, Spanish moss) in coastal Georgia (Southeastern USA). Bacteria concentrations and fluxes were greater in stemflow relative to throughfall. However, throughfall delivers water to a larger land area (ha) resulting in throughfall producing the greatest proportion of bacteria annual flux (cells ha^{-1} $year^{-1}$). Annual total (throughfall + stemflow) bacterial flux was 3.4 quadrillion cells $year^{-1}$ ha^{-1}. Roles of this previously unquantified bacterial flux to the forest floor may be significant by contributing functional community members (if living) or labile lysates (if dead) to soil communities.

Bacterial community structure was also characterized via Illumina MiSeq sequencing and

plotted for relative abundance and diversity throughout the sampling period. The predominant phyla present in rainfall, throughfall, and stemflow included *Proteobacteria*, *Bacteriodetes*, *Firmicutes*, *Actinobacteria*, and *OD1*. Taxa transported from the phyllosphere to throughfall- and stemflow-receiving soils (a) resembled biological aerosols, (b) did not significantly differ between canopy flowpaths, (c) were not influenced by the presence/absence of arboreal epiphytes, but (d) varied substantially among storms of differing air mass provenance and trajectory. Findings indicate local phyllosphere communities may not be disturbed by rainfall up to high intensities (31 mm h^{-1}). To the author's knowledge, this is the first assessment of the quantity, composition and structure of bacteria exchanged between the phyllosphere and pedosphere during rainfall, despite storms being critical biogeochemical events in forest ecosystems. Should the bacteria transported by throughfall and stemflow be able to access or establish microbial communities at the forest floor, there may be broad biogeochemical implications for the litter layer and topsoil. Thus, we suggest future research assess the fate and potential function of throughfall and stemflow bacterial communities at the forest surface.

INDEX WORDS: Throughfall, Stemflow, Epiphytes, Next-generation sequencing, Bacterial communities, Quercus virginiana

QUANTIFICATION AND CHARACTERIZATION OF NET PRECIPITATION BACTERIAL FLUX FROM A SUBTROPICAL EPIPHYTE-LADEN OAK FOREST

by

PRESTON THOMAS POUND

B.S., Auburn University, 2015

A Thesis Submitted to the Graduate Faculty of Georgia Southern University in

Partial Fulfillment of the Requirements for the Degree

MASTER OF SCIENCE

STATESBORO, GEORGIA

QUANTIFICATION AND CHARACTERIZATION OF NET PRECIPITATION BACTERIAL FLUX FROM A SUBTROPICAL EPIPHYTE-LADEN OAK FOREST

by

PRESTON THOMAS POUND

Major Professor:	John T. Van Stan, II
Committee:	Tiehang Wu
	J. Scott Harrison

Electronic Version Approved:
December 2017

ACKNOWLEDGMENTS

I would like to thank my lab mate Ansley Whitetree for assistance in the lab. I would like to thank Dr. Thais Bittar at the Skidaway Institute of Oceanography for assistance with bacterial enumeration. Finally, I would like to thank Dr. Elizabeth Ottesen and her doctoral student, Morgan Teachey, at the University of Georgia for their assistance with DNA sequencing. This research was supported by the United States National Science Foundation (DGE-0841146).

TABLE OF CONTENTS

Page

LIST OF TABLES

LIST OF FIGURES

CHAPTER 1

INTRODUCTION

Vegetation significantly alters the amount and pattern of mass and energy inputs to the land surface. Above-ground plant surfaces—leaves, bark, and epiphytes (collectively called the phyllosphere)—also arguably represent the largest terrestrial habitat as it is estimated to be greater than 6.4×10^8 km^2 (Morris and Kinkel, 2002) which is over twice the area of the global land surface (Vorholt, 2012). Microbes flourish in the phyllosphere, with previous work finding bacteria (Redford et al., 2010), fungi (Kembell and Mueller, 2014), and archaea (Finkel et al., 2011) present, but bacteria generally dominate (Andrews and Harris, 2000). The phyllosphere bacterial community is structurally and functionally diverse, enabling this community to play major roles in plant ecophysiological functioning (Lambais et al., 2006; Bringel and Couée, 2015). Because of this, much recent attention has been placed on how phyllosphere bacterial communities affect plant-atmosphere interactions (Bringel and Couée, 2015). In contrast, no studies known to the author have examined how plant-atmosphere interactions during rainfall (a critical event for biogeochemistry) may link the phyllosphere bacterial community to plant-soil interactions.

The phyllosphere is a dynamic and difficult meteorological environment as microbes are subjected to high levels of UV radiation and drastic shifts in temperature, humidity and leaf wetness (Hirano and Upper, 2000). Plant surfaces add to the inhospitable meteorological conditions by limiting nutrient availability on the phyllosphere to the point of creating a nutrient-poor, or oligotrophic, habitat (Leveau and Lindow, 2001). This is especially true where plant

surface appendages are highly efficient in scavenging water and macronutrients (Vorholt, 2012), like observed for the trichome scales of various arboreal epiphytic vascular plants (i.e., *Tillandsia* spp.). Consuming leached solutes from plant surfaces during rainfall is also difficult for the phyllosphere bacterial community as rainwater entrained on the canopy can be enriched in salts (Gay et al., 2015) and allelopathic organic compounds (Bischoff et al., 2015). Indeed, rainfall may be a significant disturbance to the phyllosphere bacterial community, physically scouring the phyllosphere with a salty, allelopathic solution.

When rainfall contacts forest canopies, it is partitioned by the phyllosphere into throughfall, stemflow, and interception loss (Levia et al., 2011). A portion of rain is intercepted (i.e., stored and evaporated) by the canopy, then what drips from the canopy or passes through gaps is throughfall and what flows down the stem is stemflow—see Section 2.1. for quantitative comparison of these rainfall partitions. Throughfall and stemflow can rapidly scour the phyllosphere with 10 to >100 L over a single storm (Levia et al., 2011) in shorter than 0.25 h (Keim and Skaugset, 2004). Prior work has found throughfall and stemflow carry anything attached to the phyllosphere: dry deposited aerosols (Van Stan et al., 2012), pollen (Lee et al., 1996), extrafloral nectar (Campbell et al. 2013), insect frass and honeydew secretions (Michalzik, 2011), and fungal spores (Sridhar and Karamchand, 2009). However, no prior work has investigated whether and to what extent throughfall and stemflow transport bacteria, one of the most abundant organisms in the phyllosphere, despite long-standing research finding millions of bacteria cm^{-2} of leaf surface (Lindow and Brandl, 2003). Furthermore, no work has examined whether the bacterial communities transported by stemflow (primarily flowing along bark) and throughfall (primarily flowing along leaves and arboreal epiphytic plants) differ as a result of the

different phyllosphere communities on bark, leaves, and arboreal epiphytic plants.

Arboreal epiphytic plants alter the interchange between throughfall, stemflow, and interception loss, as well as the composition of materials throughfall and stemflow transport (Van Stan and Pypker, 2015). Surfaces of arboreal epiphytic plants have also been found to select for unique phyllosphere microbial communities (Brighigna et al., 1992; Puente and Bashan, 1993; Fürnkranz et al., 2008). Thus, this thesis will not only examine how much bacteria and which bacterial species are carried from forest canopies to the surface by throughfall and stemflow, but will also assess whether, and to what extent, the presence of *Tillandsia usneoides* (an abundant arboreal epiphytic plant at the study site) alters throughfall and stemflow bacterial flux and community composition. Quantification and characterization of bacterial fluxes to the forest surface during storms, which are, arguably, one of the most biogeochemically active periods for ecosystems (Hinton et al., 1997), will expand our understanding of matter transport during biosphere-atmosphere interactions. It is important to note that we refer to epiphytic bacterial communities as "phyllosphere bacterial communities" and arboreal epiphytic plants as simply "epiphytes" throughout this thesis. Throughfall and stemflow will be abbreviated to TF and SF, respectively. This thesis seeks to address the following questions, objectives and hypotheses:

Question 1. What is the annual flux of bacteria via TF and SF?

Objective 0. Quantify TF and SF hydrologic fluxes for computing bacterial cell fluxes.

Objective 1. Quantify TF and SF bacterial concentrations and flux using flow cytometry.

Hypothesis 1a. Bacterial concentrations will be greater for SF versus TF. This is due to a funneling effect of the tree canopy to TF. Bacteria will be subjected to longer amounts of

contact with rainfall and be more likely to be washed from plant surfaces.

Hypothesis 1b. Flux of bacteria will be greater for TF than SF. TF makes for a large portion of rainfall partitioning because of the large amount of surface area that the tree canopy occupies. Bacteria will be easily removed from plant surfaces and epiphyte coverings during rainfall compared to SF.

Hypothesis 1c. Annual flux in cells per hectare will be significantly larger for (net rainfall) both TF and SF, compared to gross rainfall. Aerosolized bacteria will come in contact with epiphytes and plants surfaces of *Quercus*. These bacteria are easily and rapidly transported through wind and other meteorological events including fog. This wide dispersal of bacteria in *Quercus* leads to large amount of flux in forest systems.

Question 2. What is the composition of the bacterial community transported by TF and SF?

Objective 2. Apply Illumina MiSeq high-throughput sequencing of 16S rRNA genes to identify and group bacterial Operational Taxanomic Units (OTUs) in TF and SF.

Hypothesis 2. Bacterial community composition will differ significantly between rainfall, TF and SF. The bacterial communities have different plant surfaces with which they interact. The conditions for growth in the canopy frequently contributing to TF will have epiphytes, which bacteria will reside in due to high moisture and nutrient content. Bacteria utilizing bark surfaces for growth in SF will have access to different nutrients, this difference in nutrients will ultimately select for different bacterial communities.

Question 3. Does epiphyte presence alter TF bacterial flux or community composition? Note: no "bare canopy" conditions for SF from oaks could be found at the study site.

Objective 3. Compare bacterial community sequencing data for TF collected beneath bare and epiphyte forest cover.

Hypothesis 3a. Epiphyte cover will increase bacterial concentrations in both TF and SF, yet the increased interception loss from *T. usneoides* will reduce water fluxes. The net effect will be diminished TF and SF bacterial flux from canopy hosting the epiphyte.

Hypothesis 3b. Bacterial community composition will significantly differ between bare canopy- and epiphyte-derived TF as epiphyte surfaces select for unique bacterial communities compared to host leaves.

CHAPTER 2

LITERATURE REVIEW

2.1 Partitioning of Rainfall by Oak Forest Canopies

Rain falling on a forest initiates a series of significant ecohydrological processes, the very first of which involves the canopy partitioning droplets into interception, TF and SF (Levia and Frost, 2003; 2006; Carlyle-Moses and Gash, 2011). As described in the introduction, during canopy rainfall partitioning droplets can (1) drip off of plant surfaces and fall through gaps (TF), (2) be funneled down the tree's stem (SF), or (3) be evaporated back into the atmosphere (interception). Rainwater that reaches the forest floor, basically the sum of TF and SF, is called net precipitation. Of all tree genera, oaks (*Quercus*) are one of the most well-researched with regard to their partitioning of rainfall. This may, in part, be due to *Quercus* species' strong ties to human civilization and broad representation/diversity across the Northern Hemisphere (Hogan, 2012). Indeed, rainfall partitioning has been measured and modeled for temperate *Q. robur* and *Q. serrata* from Asia to Europe (Silva and Okumura, 1996; Bittner et al., 2010), as well as for tropical *Q. copeyensis* (Hölscher et al., 2004), Mediterranean *Q. ilex* (Pereira et al., 2009), montane *Q. pubescens* (Muzylo et al., 2012), humid temperate *Q. castaneifolia* in Iran (Bahmani et al., 2012), and even the semi-arid scrublands dominated by *Q. glaucoides* (Carlyle-Moses, 2004).

The northern-most reaches of *Quercus* species studied by canopy ecohydrologists are found in the temperate climate, where the majority of rainfall reaches the surface as TF—72% (Table

1). Temperate *Quercus* species had similar rainfall partition percentages, but *Q. castaneifolia* was a notable exception with SF percentages being less than 1%, while other species of this climate were higher (Table 1). In Mediterranean (and montane) climates, *Quercus* species exhibited larger variations between SF, TF and interception percentages, particularly *Q. ilex*, which ranged from 59-78% for TF partitioning, and *Q. cerris,* which had dynamic ranges for all rainfall partitions (Table 1). A review of Mediterranean rainfall partitioning studies (Llorens and Domingo, 2007) found that differences in TF, SF, and interception are generally related to stand structural conditions. It was generally reported that SF was more variable than TF, likely due to wind and other storm variables (Silva and Okumura, 1996). Denser canopy cover increases the chance for interception of rainfall (Llorens and Domingo, 2007). TF percentages appear to have

Table 1. Summary of rainfall partitioning into interception (I), throughfall (TF), and stemflow (SF) for select oak species in a variety of climates with different mean annual rainfalls (MAR).

Climate	Species	MAR (mm)	I (%)	TF (%)	SF (%)	Study
Montane	*Q. pubescens*	552.8	17.0	81.2	1.8	Muzylo et al. (2012)
Temperate	*Q. serrata*	2,140	22	72	5	Silva & Okumura (1996)
	Q. acutissima	442	25	72	3	Toba & Ohta (2005)
	Q. robur	158	21	72	4	Bittner et al. (2010)
	Q. castaneifolia	651.5	24.6	75	0.40	Bahmani et al. (2012)
Mediterranean	*Q. pubescens*	1,021	15-26	74-85	0.3	Iovino et al. (1998)
	Q. coccifera	404	-	55	-	Abdelli (1999)
	Q. pyrenaica	625-1,057	13-16	83-86	0.6-0.9	Moreno et al. (2001)
	Q. petraea	748	7	88	5	Mosello et al. (2002)
	Q. ilex	755-1,275	13-36	59-78	0.6-12	Llorens & Domingo (2007)
	Q. cerris	563-1,102	2-68	26-87	0.3-11	Llorens & Domingo (2007)
Semiarid/Arid	*Q. glaucoides*	635	12	80	8	Carlyle-Moses (2004)
	Q. ilex	432	13	75	12	Llorens & Domingo (2007)
	Q. brantii	474	30	70	<0.1	Fathizadeh et al. (2013)
Subtropical	*Q. virginiana*	523	25	71	3	Thurow et al. (1987)
	Q. virginiana	1,074	37	63	<0.1	Van Stan et al. (2016a)
Tropical	*Q. copeyensis*	2,812	29	69	2	Hölscher et al. (2004)

a positive correlation with rainfall intensity. Tree height can influence rainfall partitioning, negatively correlating with TF percentages (Llorens and Domingo, 2007). *Quercus ilex* was studied in both Mediterranean and Semi-arid climates, with the partitioning percentages being similar to one another in the higher ranges of TF, lower range of interception and SF from Mediterranean species (Table 1).

In the subtropical southeastern US, our study species (*Quercus virginiana*) has been studied with regard to partitioning of rainfall (Thurow et al., 1987; Gay et al., 2015; Van Stan et al., 2016a; 2016b). SF is very low (ultimately negligible) at this thesis' study site (<0.1%; Table 1), but Thurow et al. (1987) found SF from *Q. virginiana* could achieve as much as 3% of rainfall (Table 1). TF is around 60% (Gay et al., 2015; Van Stan et al., 2016a) and interception losses tend to be higher than other reported subtropical *Q. virginiana* (Thurow et al., 1987), due to heavy epiphyte cover consisting mainly of Spanish moss (*Tillandsia usneoides*) (Van Stan et al., 2016b).

Tillandsia usneoides is not unique in its alteration of rainfall partitioning processes via absorbing significant rainfall, disrupting channels along branches and leaves, and diverting water from the drainage pathways as this has been shown for lichen, bryophyte, and other vascular epiphytes (Schlesinger and Marks, 1977; Carroll, 1980; Van Stan and Pypker, 2015). As *T. usneoides* cover is quite large on *Q. virginiana* canopies in the subtropics and tropics (0.2 to > 3 kg biomass m^{-2} canopy area: Schlesinger, 1978; Van Stan et al., 2015), TF has been found to diminish (Gay et al., 2015). The absorption of water in conjunction with the disruption of branchflow pathways have been shown to decrease SF dramatically (Van Stan and Pypker, 2015). This increase in interception loss, and prevention of SF generation, is likely because the

average water absorbency for *T. usneoides* is approximately 800% of dry weight, resulting in a mean water storage of 4.1 ml cm^{-3} of biomass (Van Stan et al., 2015).

2.2 Solute Concentrations and Fluxes from Stemflow and Throughfall

The movement of solutes from the forest canopy to the soil is critical for soil solution chemistry (Chang and Matzner, 2000), soil formation processes (Li et al., 2009), bedrock weathering (Backnäs et al., 2012), and microbial communities structure (Rosier et al., 2015; 2016) and functioning (Moore et al., 2016), allowing net rainfall to alter understory vegetation patterns in oak forests (e.g., Andersson, 1991). Current and historical research has found that solutes in TF and SF come from three sources: (1) atmospheric deposition, (2) leaching from canopy tissues, and (3) transformations of solutes during rain droplets' transit through the canopy. This section will review the TF and SF concentration and flux of solutes reported for *Quercus* species in select studies and discuss each solute's most common sources.

The most abundantly leached solute carried by both TF and SF is K^+ (Table 2) and is thought to be contributed to rainwater from the intercellular spaces within leaves (Van Stan et al., 2012). Mg^{2+} is also readily leached from leaves, but is often found in concentrations and fluxes below K+ (Table 2). Ca^{2+} is generally thought to enter TF and SF by being leached from the cellular membranes and pectates of bark and leaf surfaces (Berger et al., 2000). It is also important to note that K^+, Mg^{2+}, and Ca^{2+} are all found in soluble salt aerosols typically related to maritime air masses (Savoie and Prospero, 1980). The most abundant sea salt aerosols deposited on tree surfaces and washed off during rainfall are Na^+ and Cl^-, resulting in these salts achieving high concentrations (Table 2). SO_4^{2-} in TF and SF is primarily from atmospheric deposition of

sulfurous gasses and particulates that settle on foliar and bark surfaces (Boxman et al., 2008). The mechanisms of sulfur deposition and washoff are complex (Ivens et al., 1990) and can modestly enrich TF and SF (Table 2). When TF and SF become highly enriched in sulfurous compounds it can result in soil acidification (Alewell, 2001). NO_3^- and NH_4^+ are commonly found to be leached into soils through continual depositions onto plant surfaces (Kristensen et al., 2004). Since NO_3^- is more tightly conserved by canopy tissues than NH_4^+ (Van Stan et al., 2012), it is often >50% less concentrated in TF and SF comparatively (Table 2). Dissolved organic carbon (DOC) fluxes to the soil are typically associated with leaf leaching and washing events (Tukey, 1970), and can be highly enriched in oak SF (Table 2) compared to all other DOC fluxes in terrestrial ecosystems (Neff and Asner, 2001). PO_4^{3+} is the least concentrated, lowest flux measured for dissolved macronutrient ions in natural *Quercus* forests (Table 2) and typically found aerosolized and then transferred to plant surfaces (Mahowald et al., 2008). The smallest concentration for any macronutrient is dissolved organic N (Table 2), which is typically derived from freshly decomposed organics in the canopy. Fluxes of rare earth elements and metals are quite low for natural oak forests (Table 2) and are deposited by multiple sources including dry fallout and fog (Avila and Rodrigo, 2003).

Epiphyte presence can alter solutes in precipitation (Table 2). K^+ has been observed to be uptaken by epiphytes in a variety of ways (Hauck and Gross, 2003; Asplund et al., 2015), but vascular epiphyte assemblages have been shown to leach more K^+ than is taken up (Van Stan and Pypker, 2015a). Ca^{2+} and Mg^{2+} have both been shown to leach into net precipitation. NH_4^+ is quickly converted to organic compounds (DON) by epiphytes due to the toxicity of NH_4^+ (Van Stan and Pypker, 2015a). As for REE in TF and SF, the rough surface of the epiphytes aid in the

capture of aerosolized metals and other ions. In fact, Rodrigo et al. (1999) indicated epiphytic uptake of heavy metals reduced contaminants in TF deposition beneath an urban oak forest. The same rough epiphyte surfaces that capture REE, also capture great amounts of sea salt aerosols like Na^+ and Cl^- (Gay et al., 2015). The result of atmospheric deposition, canopy leaching, and transformation, TF/SF develop distinct solute concentrations/fluxes (Eaton et al., 1973).

Table 2. Mean annual concentration and annual flux of select solutes representing most nutrients and metals for Quercus species from past literature. Epiphyte effect shown as an arrow indicating whether epiphytes tend to increase (↑) or decrease (↓) solute concentrations. The mechanism causing the increase or decrease is represented by a letter: D (capture of aerosols), L (leaching), U (uptake), and T (transformation). [1] From review (Van Stan and Pypker, 2015).

	Concentration ($mg\ l^{-1}$)		Flux ($kg\ ha^{-1}\ y^{-1}$)			Epiphyte
	TF	SF	TF	SF	Study	effect[1]
Macronutrients						
K	1205	1059	16.0	0.55	Rodrigo et al. (2003)	↑D↑L↓U
Mg	510	333	2.7	0.07	Rodrigo et al. (2003)	↑D↑L↓U
Ca	922	593	12.8	0.03	Rodrigo et al. (2003)	↑D↑L↓U
NH_4	1525	970	3.7	0.08	Rodrigo et al. (2003)	↑T
NO_3	403	173	3.0	0.05	Rodrigo et al. (2003)	↑T
SO_4	314	214	8.5	0.22	Rodrigo et al. (2003)	↑D↑L
PO_4	21	14	0.6	0.01	Rodrigo et al. (2003)	↑D↓U
DOC	5.6*	78^	104*	8.3^	*Gallardo & Esteban (2000) ^Van Stan et al. (2017)	↑L↑T
DON	0.6*	3.0^	11.5*	1.9^	*Gallardo & Esteban (2000) ^Van Stan et al. (2017)	↑L↓U
Micronutrients						
Na	1196	787	5.8	0.14	Rodrigo et al. (2003)	↑D
Cl	1410	1018	15.4	0.43	Rodrigo et al. (2003)	↑D
Metals						
Cu	-	-	6.9E-03	3.0E-04	Avila & Rodrigo (2004)	↑D↓U
Pb	-	-	6.8E-03	2.0E-04	Avila & Rodrigo (2004)	↑D↓U
Mn	-	-	0.49	7.0E-03	Avila & Rodrigo (2004)	↑D↓U
V	-	-	4.3E-03	1.0E-04	Avila & Rodrigo (2004)	↑D↓U
Zn	-	-	0.17	4.8E-03	Avila & Rodrigo (2004)	↑D↓U
Ni	-	-	7.3E-03	2.0E-04	Avila & Rodrigo (2004)	↑D↓U
Cd	-	-	5.9E-03	2.0E-04	Avila & Rodrigo (2004)	↑D↓U

2.3 Stemflow and Throughfall Contributions to Particulate Matter Fluxes

The role of particulate matter in forest systems with regards to TF and SF contributions has been little studied (Levia et al., 2013), despite their relevance for the cycling of inorganic (Lequy et al., 2014), organic (le Mellec and Michalzik, 2008), and radioactive elements (Endo et al., 2015). Moreover, particulate matter concentrations and fluxes in TF and SF were not available for any *Quercus* species, requiring this review to focus on the few species where data has been reported (Eaton et al., 1978; Michalzik and Stadler, 2005; le Mellec and Michalzik, 2008; le Mellec et al., 2010; Levia et al., 2013; Lequy et al., 2014; Endo et al., 2015). As much as 12.6 billion bacteria per liter have been found attached to the particles suspended in stream water (Crump et al., 1999). TF and SF particulate matter concentrations compare favorably to those in large streams (Levia et al., 2013).

In a beech (*Fagus sylvatica*) stand of Northeastern France, total atmospheric deposition of particulates in the open was 33 kg ha^{-1} $year^{-1}$ and TF was able to concentrate these particulates by over 5 times (Lequy et al., 2014). Many of the particles carried by TF and SF were soluble, leaving only 16 and 0.3 kg ha^{-1} $year^{-1}$, respectively, of non-soluble mineral particulates to be transported to the forest floor (Lequy et al., 2014). The greatest contribution of any inorganic nutrient supply from the particulates was observed for P (17-32%), following by Mg (15-22%), K (18-19%), and Ca (<10%) (Lequy et al., 2014). SF total particulate matter flux was low despite beech being a prodigious SF producer, only making up 3% of TF particulate matter (Lequy et al., 2014). Lequy et al. (2014) also measured particulate organic matter, finding that TF concentrations were triple what was observed in the open.

Unlike inorganic particulates, organic particulates in net rainfall fluxes have been

examined for more than one species, beech (again) and Norway spruce (*Picea abies*) in undisturbed forests, and in insect infested stands composed of sessile oak (*Quercus petreaea*) and Scots pine (*Pinus silvestris*). However, no studies have reported annual concentrations and fluxes of particulate organic matter for SF. Undisturbed TF concentrations of particulate organic C were found to be 1.9 and 2.9 mg L^{-1} in beech and spruce stands, respectively (le Mellec et al., 2010). Particulate organic N TF concentrations were much lower, averaging 0.4 mg L^{-1} for beech and 0.6 mg L^{-1} for spruce (le Mellec et al., 2010). These concentrations resulted in TF fluxes of particulate organic C of approximately 17 kg ha^{-1} $year^{-1}$ regardless of the species (le Mellec et al., 2010). Particulate organic N TF fluxes were more variable between species, with beech stands generating 3.2 kg ha^{-1} $year^{-1}$ compared to 3.6 kg ha^{-1} $year^{-1}$ estimated for spruce (le Mellec et al., 2010). le Mellec et al. (2010) provides further details on the seasonal variability of TF particulate organic matter concentrations and fluxes. The largest disturbance to annual particulate organic matter concentration and flux, so far identified, has been insect infestation (Michalzik and Stadler, 2005; le Mellec and Michalzik, 2008). For Scots pine, infestation by the lappet (*Dendrolimus pini*) doubled particulate organic N and tripled particulate organic C fluxes in TF (le Mellec and Michalzik, 2008). Infestation in beech-oak and spruce stands in Germany also changed the chemical character of the particulate organic matter, increasing amino-N and hexose-C compounds from feces and honeydew secretions carried by TF (Michalzik and Stadler, 2005).

Finally, one study examined the role TF and SF played in the return of atmospheric and radioactive ^{137}Cs in a mixed maple-oak (*Acer-Quercus*) and a Japanese cedar (*Cryptomeria japonica*) stand (Endo et al., 2015). Fluxes throughout a year for the radioactive particles

measured 13.5 kBq kg^{-1} in mixed deciduous stands. Data showed that the ^{137}Cs concentrations in TF and SF were 2.1-3.9 Bq L^{-1} and 13.4-20.3 Bq L^{-1} with annual fluxes of 131.3-204.9 Bq m^{-2} and 53.8-144.4 Bq m^{-2}, respectively. The amount of radioactive ^{137}Cs flux from SF is only about 1/50 of the amount from TF. There was some interspecies differences as concentrations in SF were 1.5-6 fold higher in mixed deciduous stands than in evergreen cedar stands, likely due to a funneling effect of the canopy types of the stands (Endo et al., 2015).

2.4 Throughfall and Stemflow Transport of Microbes to the Pedosphere

Biogeochemists recognize the importance of TF and SF for the ecological functioning of macro-flora in forest systems, but few studies have investigated microbial interactions with net rainfall and all studies on microbial transport by TF and SF focus on fungal spores (i.e., conidia) (Levia and Germer, 2015). MacKinnon (1982) was the first to identify several fungal species being transported in SF. Since then, several studies have found more fungal species' conidia being transported in SF and TF (e.g., Gonczol and Revay, 2003; Sridhar et al., 2006; Magyar, 2008; Magyar and Revay, 2009). Sridhar et al. (2006) hypothesized that SF may be a way for asexual fungal conidia and spores to spread along moist vegetative surfaces. Findings from Magyar and Revay (2009) also indicate that fungal spores utilize water flowing along the tree bark for transport. In fact, fungal spores were observed in bark during dry periods, with furrows in the barks serving as a temporary storage space for spores until transport during rainfall events (Magyar, 2008).

Figure 1. Fungal conidia from stemflow and throughfall samples (Gönczöl and Révay, 2004).

2.5 Epiphytes on Epiphytes: Phyllosphere Bacterial Communities on Arboreal Epiphytic Plants.

The canopy structure of trees and diversity of tree species can produce a variety of unique surface environments (i.e., bark, leaves, epiphytes) resulting in highly variable bacterial phyllosphere communities. For example, at the broadest scale *Bacteroides* and *Betaproteobacteria* were observed to be common in gymnosperms compared to *Actinobacteria* and *Gammaproteobacteria* being more common on angiosperms (Redford et al., 2010). When epiphytes are added to the standard bark and leaf canopy surfaces, new bacteria species may settle on the epiphyte surfaces – Brighigna et al. (1999) found nitrogen transformation bacteria colonizing a *Tillandsia* epiphyte to aid in the plant's nutrient absorption. In fact N-fixing bacteria were quite dominant on *Tillandsia* leaves, with counts of total bacteria numbering 103 x 10^4 CFU/g with nitrogen fixing bacteria comprising 2.5 x 10^4 CFU/g (Brighigna et al., 1999). Species found to the *Tillandsia* phyllosphere include: *Tillandsia* included *Aeromonas spp., Agrobacterium radiobacter, Bacillus brevis, Bacillus cereus, Bacillus circulans, Bacillus licheniformes, Bacillus pumilus, Bacillus subtilis, Bulkolderia cepacea, Enterobacter*

agglomerans, Erwinia spp., Flavobacterium spp., Flavobacterium odoratum, Pseudomonas luteola, Pseudomonas maltophila, Pseudomonas paucimobilis, Pseudomonas vesicularis, Rhanella aquatilis, Serratia liquefaciens, Serratia marcescens, Sphingobacterium spp, Sphingobacterium multivorum, and Yersinia aldovae (Brighigna et al., 1999). It is also believed that bacteria are more abundant in epiphytes, as they can use the epiphyte's large surface area and moisture retention to colonize (Hirano and Upper, 2000).

Forest stands with epiphytes have been shown to have larger amounts of total nitrogen fixation compared to trees stripped of epiphytes. Bacterial DNA was found in these epiphytes, comprised of cyanobacterial homologues. Non-cyanobacterial sequences in the epiphytes included γ-proteobacteria, b-proteobacteria and a-proteobacteria (Fürnkranz et al., 2008). This is different from leaves and bark phyllosphere bacterial communities as Cyanobacteria members were not found in epiphyte coverings. Diazotrophic microbial communities existed in both bare and epiphytic plant surfaces, indicating that nitrogen fixation was occurring throughout the plant canopy with different bacterial species (Fürnkranz et al., 2008). Another study performed by Brighigna et al. (1992) found that a majority of bacterial species in *Tillandsia* are composed of *Bacillus* and *Pseudomonas* members, both of which are frequently found in tree canopy communities.

CHAPTER 3

METHODS AND MATERIALS

3.1. Study site

The following study site characteristics were used to scale water (objective 0) and bacterial observations to per hectare fluxes (objective 1). The study site is located on Skidaway Island (31.9885°N, 81.0212°W). Climate for the area is subtropical humid (Köppen Cfa), with a range of 750-1200 mm $year^{-1}$ for 30-year mean annual precipitation (GA Office of the State Climatologist, 2012). Mean monthly summer and winter temperatures are 30 to 35°C and 3 to 10°C, respectively (GA Office of the State Climatologist, 2012). Elevation ranges from 0 to 10 m above mean sea level. The forest sampling site is flat (0-5% slopes), underlain by Chipley fine sandy soils (Natural Resources Conservation Service-Web Soil Survey, 2015), and populated primarily by *Quercus virginiana* Mill. (Southern live oak) in the interior and by *Juniperus virginiana* L. (Eastern red cedar) along the edge (Table 3). Both species host dense epiphyte cover by *Tillandsia usneoides* L. (Spanish moss) and *Pleopeltis polypodioides* (resurrection fern), ranging from 24 to 45% of canopy coverage per spherical densiometer estimates (Table 3). Total stand density is moderate (under 500 stems ha^{-1}) and oak dominates in number of trees as well as basal area (Table 3).

Table 3. Stand structural characteristics for oak at the Skidaway Island forest.

Metric	Units	Oak
Stand density	stems ha^{-1}	315
Mean diameter at breast height (dbh)	cm	40.5
Trunk area	m^{-2} ha^{-1}	59.3
Gap fraction	%	26
Leaf Area Index (LAI)	m^2 m^{-2}	3.9
Epiphyte coverage	%	24

3.2. Hydrometeorological methods and sample collection:

Water samples across the common storm conditions experienced at the site needed to be collected for the comparison of bacterial flux throughout the calendar year (Objective 0). Seventeen storms were measured between October 2015 and September 2016, representing the typical range of storm sizes (7-74 mm event^{-1}), intensities (1-31 mm h^{-1}), and antecedent dry periods (22-400 h) for the study site (see Section 4.1. for details). In addition to storm magnitude, intensity, wind characteristics, and antecedent dry period, 48 hour back-trajectories of synoptic scale air mass movements were determined from the US National Oceanic and Atmospheric Administration's HYSPLIT atmospheric transport and dispersion modeling system (Stein et al., 2015). HYSPLIT trajectory calculations were conducted using the online model under "normal" trajectory type settings with Global Data Assimilation System (GDAS) 0.5 meteorology and level 1, 2, and 3 height settings of 500, 1000, and 1500 AGL. Resulting trajectory data show a wide range of storm origins, directions of travel, and scatter between origins of 500, 1000, and 1500 AGL air mass movements.

For each storm, three bulk rainfall samples were collected in an open area immediately adjacent to the TF and SF monitoring and sampling area. Twelve TF samplers (0.18 m^2, 0.5 m height, high density polyethylene (HDPE) bins) were deployed immediately before each storm beneath *Q. virginiana*. All samplers were pre-cleaned with ultrapure water (Milli-Q, Millipore) acidified to pH 2 with trace clean 6N HCl, then triple-rinsed with ultrapure water, air dried, and covered until the start of a rainfall event. The bins were distributed to represent epiphyte-covered and bare canopy areas. Four SF samplers were installed on *Q. virginiana* trees consisting of polyethylene tubing collars wrapped about the trunk at 1.4 m height and connected to 120 L

HDPE bins. TF and SF volumes were measured manually during sample processing. Within 8 hours after a storm, samples were collected and processed for flow cytometry and quantitative Polymerase Chain Reaction (qPCR) assays. All sampling and sample processing materials (syringes, filters, and bottles) were pre-cleaned with acidified ultrapure water, triple-rinsed with ultrapure water, then triple-rinsed with a small amount of sample.

3.3. Flow cytometry:

For flow cytometry, samples were collected into 5 mL cryovials, preserved with 0.1% glutaraldehyde solution (final concentration) and frozen at -80 ºC until analysis (Objective 1). Samples were vigorously vortexed in an attempt to break apart and release particle-attached bacteria, and passed through a 50 µm mesh to preclude the introduction of larger particles into the flow cytometer cell. Thus, bacterial concentrations obtained by this method refer to 'free bacteria' and do not include particle-attached cells that could not be disrupted by vortexing. Bacterial concentrations in SF, TF and rainfall samples were determined by DNA-specific staining with Sybr Green I (1x final concentration) and enumerated using a FACSCalibur (BD Biosciences) or a Guava (Millipore) flow cytometer. Blanks consisted of 0.22 µm-filtered water aliquots, stained and analyzed as described above. Staining was performed according to published methods (Marie et al., 1997; Bittar et al., 2016) and optimized for rain, TF and SF samples. Fluorescent polystyrene beads (1 µm, Spherotech) were used to account for instrument reproducibility. Both flow cytometers are equipped with a 15 mW air-cooled argon-ion laser tuned for blue excitation (ex 488 nm) with emission detectors at 535, 585 and 650 nm, and forward and side scatter light detectors. Samples from the storm underwent flow cytometry to

determine the concentration of cells from the storm. The samples were fixed with glutaraldehyde following the storm for preservation purposes then stored at -80°C to prevent denaturing of the cells before flow cytometry can occur until they are ready for flow cytometry analysis. The samples prepared for flow cytometry were run through a 50µm filter to remove detritus from the vials they were stored in. 100µL of the sample will be mixed with 98µL of MilliQ water and then stained with 1X SYBR Green. The samples were run in the flow cytometry machine (Guava easyCyte Flow Cytometer, MilliporeSigma) at Skidaway Island Institute of Oceanography (SkiO) and the data was collected on the cellular concentrations of each storm.

3.4. DNA extraction:

DNA extraction from water samples was necessary for qPCR (Objective 1) and Illumina sequencing (Objective 2). Rainfall, TF and SF samples were processed by taking 60mL from the collectors and filtering the water through an Acrodisc Syringe Filter with GHP Membrane. These filters were frozen immediately at -80°C and transported back to Georgia Southern University for DNA extraction. The DNA extraction was performed using the MO BIO PowerWater Kits from QIAGEN. The protocol used for DNA extraction followed the MO BIO PowerWater kits available from the company's website. However, the protocol was slightly modified, using a Dremel tool to extract the filter membrane and then placed directly into the Bead Tubes. The Dremel tool was used due to the relative difficulty to separate the halves of the filter. Following DNA extraction, the samples were kept at -20°C before shipment for sequencing.

3.5 Quantitative PCR (Q-PCR)

The samples underwent qPCR to validate flow cytometry bacteria concentrations required to address objectives 1 and 2 The protocol for qPCR is as follows: Per sample, the master mix for the reaction is 10µL of colorless 1X TAQ polymerase, 0.8µL of 10µM 16S forward primer (1070F), 0.8µL of 10µM reverse primer (1392R), 2µL of 1X SYBR green and 4.4µL of water. The mix will be adjusted for 18µL of master mix and 2µL of sample for the reaction. Samples will be loaded onto a 96 well plate and run through a PCR machine. The reaction underwent an initial phase of 5 min at 94ºC; 40 cycles of 1 min at 94ºC, 30s at 61ºC, and 1 min at 72ºC; and 10 min at 72ºC. The 1070F and 1392R primers were used in this study because they are universal bacterial primers, as we are concerned with only bacterial microbes in this aspect of rainfall depositions. Standards were created from 1 to 10-fold dilutions from bacterial samples of known concentrations amplified using 1070F and 1392R primers. Efficiencies were 87-100%. Melt curve analysis was captured at the end of the 40^{th} cycle for end of run analysis and cycle threshold values and gene abundance were taken from the end of the 40^{th} cycle.

3.6 Illumina DNA Sequencing:

The 16S rRNA gene in every collected rain, TF, and SF sample was amplified in duplicate per a 2-step PCR method based on Caporaso et al. (2010) (Objective 2). First PCR consisted of Q5 Hot Start high-fidelity DNA polymerase (New England BioLabs, Ipswich, MA) and 515F (GTGCCAGCMGCCGCGGTAA) and 806R (GGACTACHVGGGTWTCTAAT) primers in a 10 µL PCR mixture (1x Q5 reaction buffer, 200 µM deoxynucleoside triphosphates

[dNTPs], 0.5 μM 515F, 0.5 μM 806R, 2 ng DNA, and 0.02 U/μL Q5 polymerase) at 98°C for 30 s, followed by 15 cycles at 98°C for 10 s, 52°C for 30 s, and 72°C for 30 s, with a final extension step at 72°C for 2 min. Immediately after this initial reaction, the resulting product was reamplified using primers (see Table S1 from Tinker and Ottesen [2016]) that contained double Hamming barcodes. This two-step PCR ensures high quality amplicons, since initial replication occurs prior to the addition of Illumina-specific adaptors or sample-specific barcodes (Tinker and Ottesen, 2016). Secondary amplification mixture contained 1 x Q5 reaction buffer, 200 μM dNTPs, 0.5 μM 515F, 0.5 μM 806R, 2 ng DNA, and 0.02 U/μL Q5 polymerase. 21 μL was added from this mixture to 9 μL of the initial reaction product. These reactions were then cycled at 98°C for 30 s, followed by 4 cycles at 98°C for 10 s, 52°C for 10 s, and 72°C for 30 s, followed by 6 cycles at 98°C for 10 s and 72°C for 1 min, concluding with a final extension at 72°C for 2 min. Two independent PCRs with unique barcode combinations were generated for each sample, then these technical replicates were pooled and purified using the EZ Cycle Pure kit (Omega Bio-tek) according to the manufacturer protocol. Samples were eluted in 30 μL of elution buffer. Purified amplicons were quantified using a NanoDrop Lite spectrophotometer (Thermo Scientific). Quality of the prepared library was assessed on an Agilent 2100 Bioanalyzer DNA-HS assay (Agilent Technologies, Santa Clara, CA), then submitted to the Georgia Genomics Facility for sequencing (Illumina MiSeq 250 bp; Illumina, Inc., San Diego, CA).

3.7. Data analysis:

As rainfall, TF and SF data are skewed, nonparametric descriptive statistics are presented and nonparametric statistical tests were applied. For “objective 0,” there are no explicit

hypotheses, thus, rainfall, TF, and SF were simply described using standard descriptive statistics (median ± interquartile range). Statistical comparisons using cell count and qPCR data were performed using the nonparametric Mann-Whitney test with $p < 0.05$ in Statistica 12 (Statsoft, OK, USA). To test hypothesis 1a, median bacteria concentrations for TF versus SF were computed from event-scale data and compared. Hypothesis 1b was tested comparing median bacteria flux per unit rainfall and per unit time as calculated with infiltration area from Table 3 (m^2), event rain amount (mm) and event duration (h); yielding units of cells m^{-2} mm^{-1} and cells m^2 h^{-1}, respectively. Hypothesis 1c was tested by comparison of annual bacterial fluxes (cells ha^{-1} $year^{-1}$) scaled by multiplying annual rainfall amounts (mm) for 2014, 2015, and 2016 with median bacterial flux per unit rainfall (cells m^{-2} mm^{-1}). Hypothesis 3a was tested by statistical comparisons of median bacterial concentrations between bare and epiphyte-covered TF.

Assessment of hypotheses 2 and 3b required matching Illumina sequences to bacterial community databases using mothur software (Schloss et al., 2009) and comparison of TF versus SF community structures. The samples were processed following a modified protocol of the mothur SOP with the intention of improving accuracy and reporting, including alignment with Greengenes database and clustering operational taxonomic units (OTUs) at 97% similarity. Modifications included: after sequences were assembled, sequences that had any ambiguous bases or were longer than 275 bp were removed; sequences that passed this initial screening process were aligned to the Silva reference database (Release 123) (Pruesse et al., 2007; Quast et al., 2013; Yilmaz et al., 2014); aligned sequences were again screened to remove sequences that contained homopolymers of 8 or more base pairs; UCHIME was used for identifying chimeras from the remaining sequences (Edgar et al., 2011); after chimera removal, the Wang method was

used for taxonomic classification of samples with the greengenes reference database (August 2013 version) (Wang et al., 2007; DeSantis et al., 2006; McDonald et al., 2012); sequences that were unclassifiable or identified as chloroplasts, mitochondria, and Eukaryota were removed. The remaining sequences were clustered into OTUs on the basis of 97% or greater sequence identity. Samples with less than 5000 reads were removed from analyses (17-15,17-16,17-21). All community composition barplots made with the mothur data was plotted at the OTU level. Explicit assessment of the dissimilarity in community composition between (Hypothesis 2) rain, TF, and SF, as well as (Hypothesis 3a) epiphyte versus bare TF was done using 2 complementary statistical approaches: (1) a permutational multivariate analysis of variance (PERMANOVA) on family-level community composition, Shannon's diversity index, and Bray-Curtis dissimilarity index; (2) Nonmetric multidimensional scaling (NMDS) visualization of individual fluxes in storms. Statistical analyses on sequencing data were performed in R (R Development Core Team, 2008).

The Bray-Curtis dissimilarity and Shannon's diversity indices were computed in mothur (Kozich et al., 2013) on OTUs $\geq$ 97% per calculations detailed on the mothur wiki page:

- https://www.mothur.org/wiki/Shannon
- https://mothur.org/wiki/Braycurtis

PERMANOVA is a non-parametric multivariate test commonly used to compare community compositional differences between groups. The null hypothesis of PERMANOVA is that the center, and variability around the center, of individual communities in a data-specific measurement space is equivalent. Rejection of the null hypothesis, therefore, indicates that a community centroid and its variability is distinct from other communities in the comparison.

PERMANOVAs were executed using the vegan package in R (Oksanen, 2015). NMDS analyses were conducted to present differences in family-level community composition in two dimensions, where similarity of communities is indicated by proximity. The confidence of interpretation by proximity is represented by the "stress value", which is an estimate of how well the ordination fits the two-dimensional (in this instance) representation. Any stress value < 0.2 indicates good fit between ordination and representation (Oksanen, 2015). NMDS analyses were also performed using the vegan package in R (Oksanen, 2015).

CHAPTER 4

RESULTS – NET RAINFALL DYNAMICS

4.1. Meteorological conditions

The storms sampled throughout the study were a wide range of precipitation levels. Storms varied from less than 10 mm of rainfall to 123 mm (Figure 2). Tropical storms Hermine and Bonnie were sampled and represent the larger of the rainfall events (Figure 2). The events with the smallest amounts of rainfall were still sufficient for bacterial flux for the purposes of sampling.

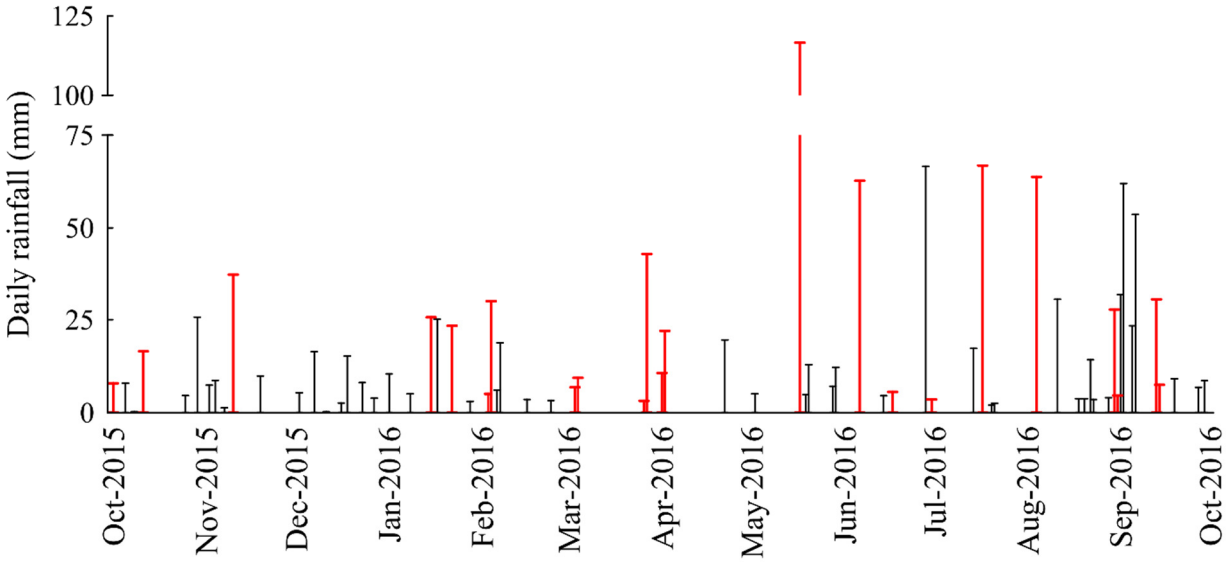

Figure 2. Daily rainfall amounts for storms sampled within the study site during the study period with the 17 sampled storms highlighted in red.

The sampled storms had a median rainfall amount of 24.5 mm. Rainfall amount had an interquartile range between 20 and 45 mm. Rainfall intensity had less of a range, with the outlier and extreme outlier representing the tropical storms previously stated. The antecedent dry period (ADP) represents the amount of hours between rainfall events, allowing for bacteria and nutrients to accumulate on plants surfaces. The ADP had large ranges, with a majority falling between 110 and 240 h. The largest ADP was short of 400 h. Smallest ADP was less than 24h.

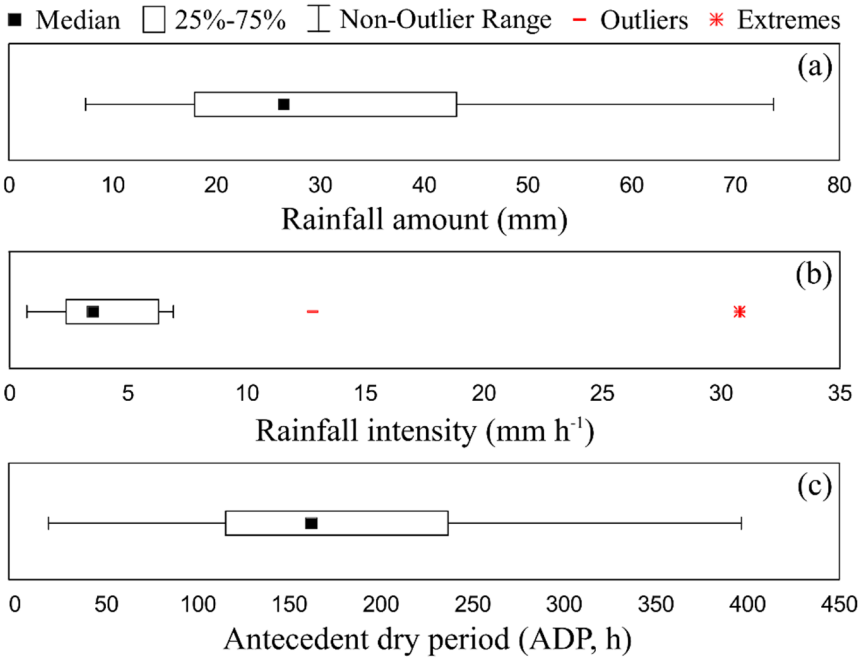

Figure 3. Conditions of sampled storms include a range of (a) magnitudes, (b) intensities, and (c) antecedent dry periods (ADP).

Storms were sampled between October 2015 and September 2016. Annual storm characteristics varied widely between rainfall amounts, storm intensity, wind speed and ADP. Storms with larger rainfall amounts on average had higher intensity. Wind speed is not correlated with storm intensity nor rainfall, but likely affected the amount of TF and SF as higher wind speed affected the amount of precipitation that came into contact with the tree canopies.

Table 4. Meteorological characteristics for the sampled storms. "ADP" stands for "antecedent dry period."

Storm Date	Storm Number	Rainfall (mm)	Intensity (mm/h)	Mean wind speed (m/s)	Max wind speed (m/s)	ADP (h)
10/1/2015	N/A	7.4	6.3	1.6	4.4	155.2
10/10/2015	N/A	17.9	6.9	1.6	5.8	118.3
11/8/2015	N/A	26.5	1.8	2.5	7.2	98.3
1/15/2016	N/A	26.5	4.7	1.6	8.1	168.6
1/22/2016	N/A	28.8	12.8	1.2	5.0	122.5
2/4/2016	N/A	50.3	2.4	1.6	8.9	164.9
3/3/2016	N/A	20.4	2.6	1.9	8.5	202.7
3/27/2016	14	34.6	0.8	1.2	6.3	119.8
4/1/2016	16	48.8	3.7	1.7	8.5	110.7
5/17/2016	17	65.8	6.4	2.2	10.3	251.6
6/6/2016	18	73.7	3.2	1.2	9.4	168.0
6/17/2016	19	14.7	3.5	2.1	14.3	246.9
6/30/2016	20	18.3	2.6	1.0	8.1	21.7
7/17/2016	21	10.9	2.2	1.4	11.6	399.8
8/3/2016	22	16.5	5.5	1.1	6.3	376.4
8/30/2016	24	33.4	30.8	5.9	15.3	63.7
9/13/2016	25	43.1	2.4	2.2	14.4	239.7

4.2. Throughfall production

TF production was not significantly affected by whether or not the trees had epiphytes in the canopies ($p > 0.1$). The range of TF amount was 15 to 40 mm for bare, 15 to 40 mm for epiphyte-covered (Figure 4). The proportion of rainfall that became TF ranged from 55 to 70 mm for bare, 60 to 80 mm for epiphyte (Figure 4). The median for TF amount in bare was 15 mm and 20 mm for epiphyte-covered TF (Figure 4).

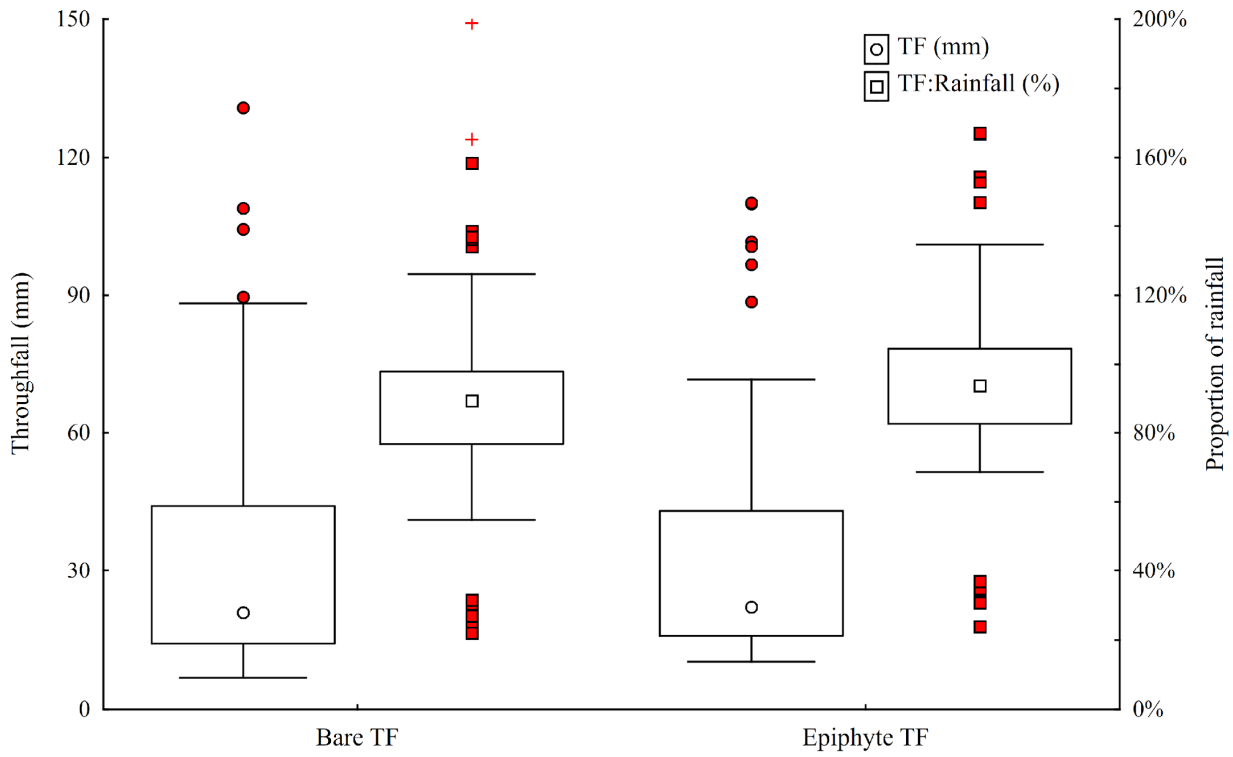

Figure 4. Median and interquartile (25%-75%) range of depth equivalent (mm) and proportion of rainfall (%) for bare canopy throughfall, and epiphyte-covered throughfall beneath Quercus virginiana.

The trend found in Figure 5 shows strong correlation between rainfall amounts and TF production. The trend is very similar between bare and epiphyte-covered canopies (Figure 5). They both have positive linear relationships (Figure 5). They both produced storms of both high and low TF productions compared to the regression at the same time (Figure 5).

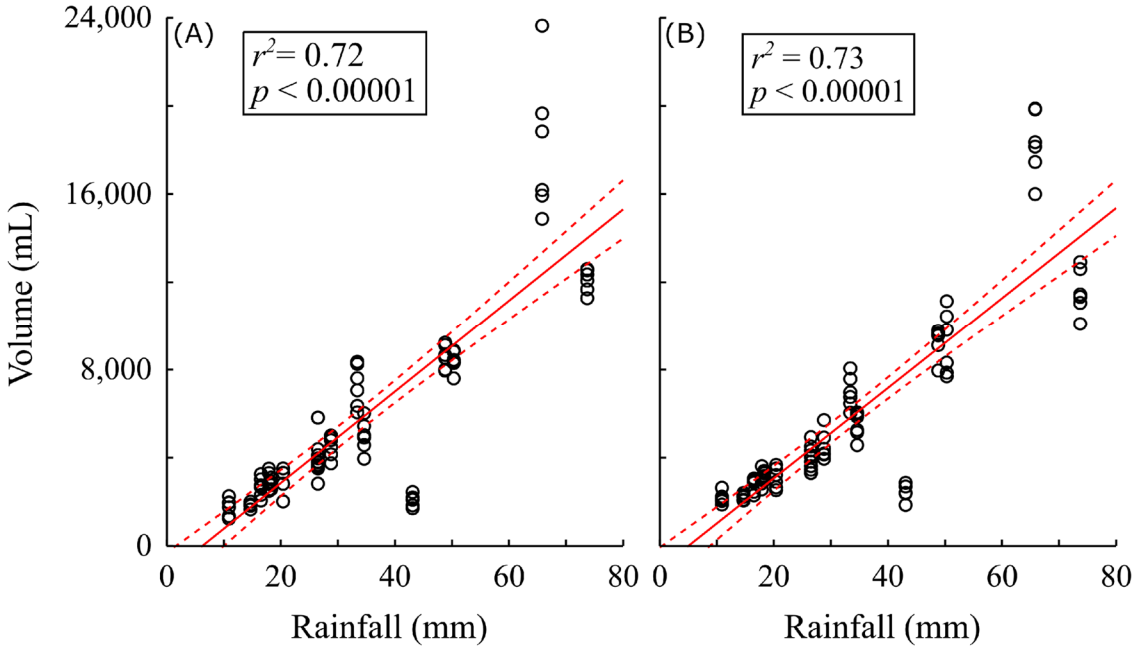

Figure 5. Plot of rainfall amount (mm) versus throughfall volume (ml), for (A) bare and (B) epiphyte covered canopy.

4.3. Stemflow generation

Median SF volume was 1.17 L storm^{-1} with an interquartile range of 0.89-3.90 L storm^{-1}. The median depth equivalent of SF received at the base of the stem was 4.7 mm storm^{-1} with a minimum of 0.4 mm and maximum of 33.8 mm within a single storm. The trend shows a strong correlation between SF volume and rainfall amounts with an r^2 generally greater than 0.57. SF trends among individual trees shows high variability, ranging up to an r^2 value of 0.79. Tree 1 had the highest regression correlation of the sampled trees for SF, while Trees 2-4 had a much lower slope and a lower r^2 value (Figure 6).

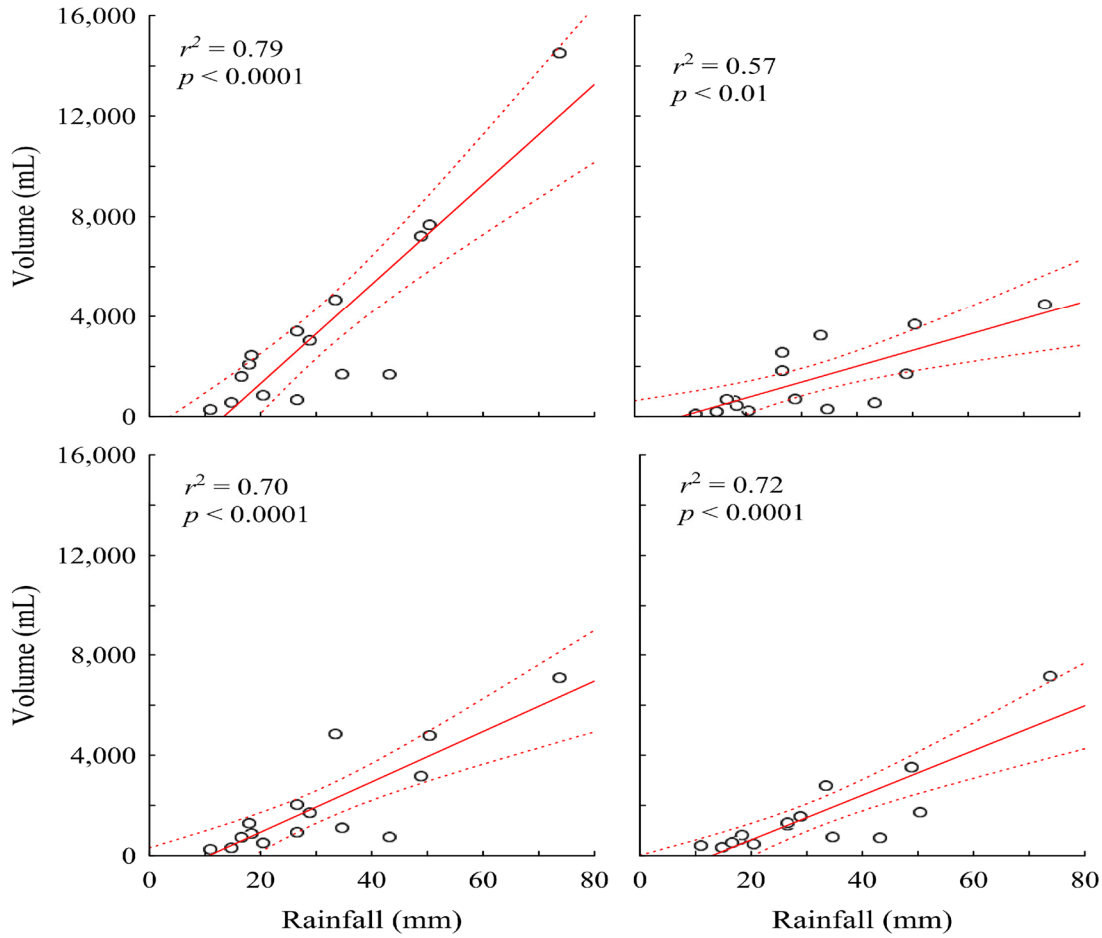

Figure 6. Stemflow relationship with rainfall amount for, in clockwise order, tree 1, 2, 4, and 3.

CHAPTER 5

RESULTS – BACTERIAL CONCENTRATION AND FLUX

5.1. Evaluation of flow cytometry with qPCR

Cell fluorescence was close to the error limits of the flow cytometer, necessitating confirmation of measurements using qPCR (Objective 0). The bacterial concentrations for the storms show that there is no significant difference between bacterial concentrations and gene abundances. A statistically significant linear regression was observed between bacterial concentration and gene copies (r^2 = 0.75: without "leverage" points >1E+6 cells mL^{-1}) (Fig. 7).

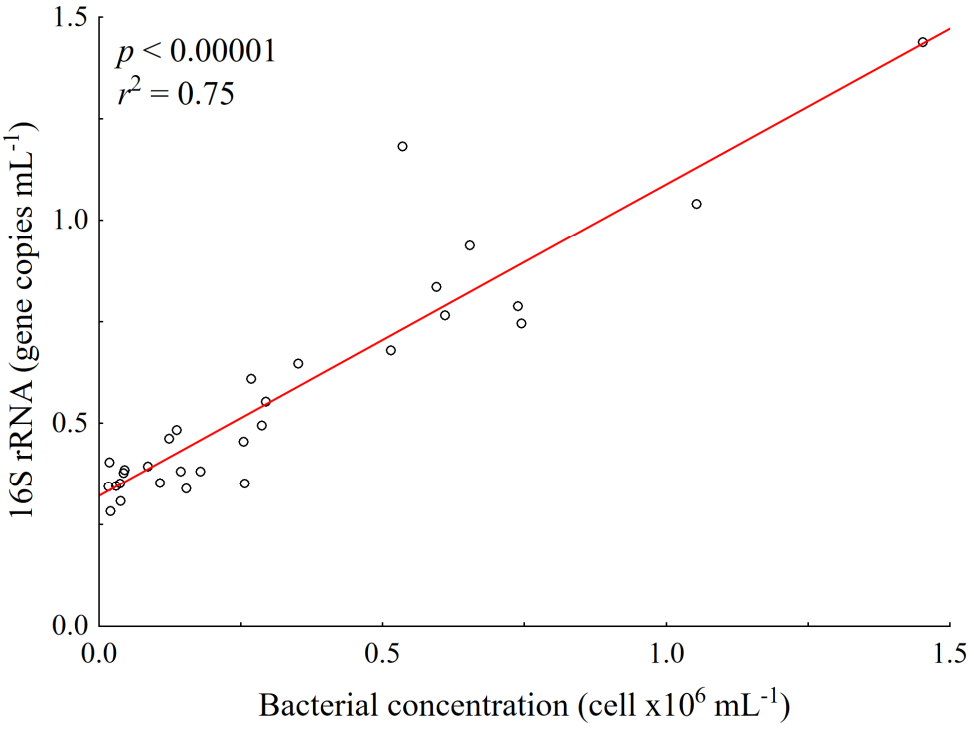

Figure 7. Correlation between bacterial concentrations (cell ml^{-1}) from flow cytometry and gene abundances measured by qPCR (copies ml^{-1}) for a subset of 51 rain samples.

5.2. Mean storm event concentration and flux

Bacterial concentrations in rainfall were the lowest of all fluxes and SF was the highest (Table 5). The concentration of these cells for SF reached up to 3.5E+05 cells ml^{-1}, with TF having a concentration of 2.2E+05. For bacterial flux in relation to time, TF was larger than SF. (Table 5). TF had a larger flux per unit of rain IQ than SF (Table 5). Rainfall measurements for concentration per unit rain were similar to SF.

Table 5. Median values of tree-derived hydrologic fluxes' bacteria concentration (cells mL^{-1}), storm-normalized bacteria flux per hour (cells m^{-2} h^{-1}) and per rainfall amount (cells m^{-2} mm^{-1}) and area-normalized bacteria flux (cells ha^{-1} $year^{-1}$) for stemflow (SF), throughfall (TF) and total (SF + TF) from oak (Quercus virginiana); and Mann-Whitney p-values for multiple comparisons with significance level at $p < 0.05$. Numbers in parenthesis are standard error; n = sample size; n/a = not applicable. Note: epiphyte versus bare TF was not significantly different ($p > 0.05$).

Tree	Flux	Cells mL^{-1} ($x10^5$)	Cells m^{-2} h^{-1} ($x10^8$)	Cells m^{-2} mm^{-1} ($x10^8$)	*n*
Oak	SF	3.5 (0.59)	1.5 (3.0)	0.38 (0.18)	59
	TF	2.2 (0.25)	6.3 (3.7)	1.8 (0.22)	187
	Total	5.7 (0.84)	7.9 (6.8)	2.2 (0.40)	246
Rainfall	R	0.52 (0.62)	1.8 (2.5)	0.52 (0.62)	36
		p-value (Mann-Whitney U test)			
Oak	SF vs TF	0.0118	<0.0001	<0.0001	n/a
Total	R vs Oak	<0.0001	0.0006	<0.0001	n/a

5.3. Annual net rainfall bacterial flux

Total annual estimates of rainfall for 2014-2015 was 1278 mm with standard error. *Quercus virginiana* at the study site was estimated to cover over 7400 m^2 ha^{-1}. TF fluxes exceeded 50 million bacteria m^{-2} mm^{-1} of rainfall. Oak SF produced multiple trillions of cells per year, while TF produced cells numbering over a quadrillion, total annual sums of bacterial fluxes in *Q. virginiana* canopies are estimated to total 1.91 quadrillion cells for the year 2015 (Table 6).

Table 6. Estimates of Annual net bacterial flux determined per 30-year Mean Annual Rainfall (MAR), 2014 and 2015.

Condition	Rain	SF	TF	SF+TF	Net Rainfall
30-year MAR:	1.28E+14	2.68E+12	1.29E+15	1.29E+15	1.42E+15
2014:	1.45E+14	3.03E+12	1.46E+15	1.46E+15	1.61E+15
2015:	1.72E+14	3.60E+12	1.74E+15	1.74E+15	1.91E+15

CHAPTER 6

RESULTS – NET RAINFALL BACTERIAL COMMUNITY COMPOSITION

6.1. Bacterial community composition for example storms

Three example storms (6-Jun-2016, 3-Aug-2016, and 13-Sep-2016: Table 4) were selected to represent the range of bacterial communities observed in open rainfall, TF and SF samples collected beneath *Q. virginiana* canopy (Figure 8). The 6-Jun-2016 storm event represents a storm where family abundance is relatively even between rainfall, TF and SF samples (Figure 8). However, the storm on 3-Aug-2016 shows the greatest variability of diversity between sample types observed in the study (Figure 8). Bacterial communities from the 13-Sep-2016 storm represent the case where, like 6-Jun-2016, abundance is fairly similar across sample types, but a common phyla (Actinobacteria) is absent in some samples or less than 5% abundance in other samples (Figure 8).

The predominant phyla present included Proteobacteria, Bacteriodetes, Firmicutes, Actinobacteria, and Cyanobacteria (Figure 8). The even distribution of bacterial community members across sample types in the 6-Jun-2016 storm showed a high proportion of Proteobacteria, representing over a third, 35% (Figure 8). Across storms, Proteobacteria was the most abundant, in some cases exceeding 50% (Figure 8). Bacteroidetes accounted for the next largest group of identifiable bacterial families for all storms, being 15%, followed by Actinobacteria, 5-10% (Figure 8). During the storm with the greatest variability in community composition across samples, 3-Aug-2016, Bacteriodetes reached 34% in epiphyte TF (Figure 8).

Firmicutes was present in low abundances for rain, TF and most SF for 6-Jun-2016 and 3-Aug-2016, ~5%, and absent in all 13-Sep-2016 samples but one epiphyte TF sample (Figure 8). The greatest Firmicutes abundance was observed for SF on 3-Aug-2016, 44% (Figure 8). A marked difference among Proteobacteria in rainfall, SF and TF samples was that Pseudomonadacea generally accounted for a larger proportion in bare and epiphyte TF, 12%, compared to rainfall and SF, 5% or less (Figure 8). No Cyanobacteria were present in the 6-Jun-2016 or 3-Aug-2016 storms, but they represented 5-10% of the bacterial community in some bare TF samples from 13-Sep-2016 (Figure 8).

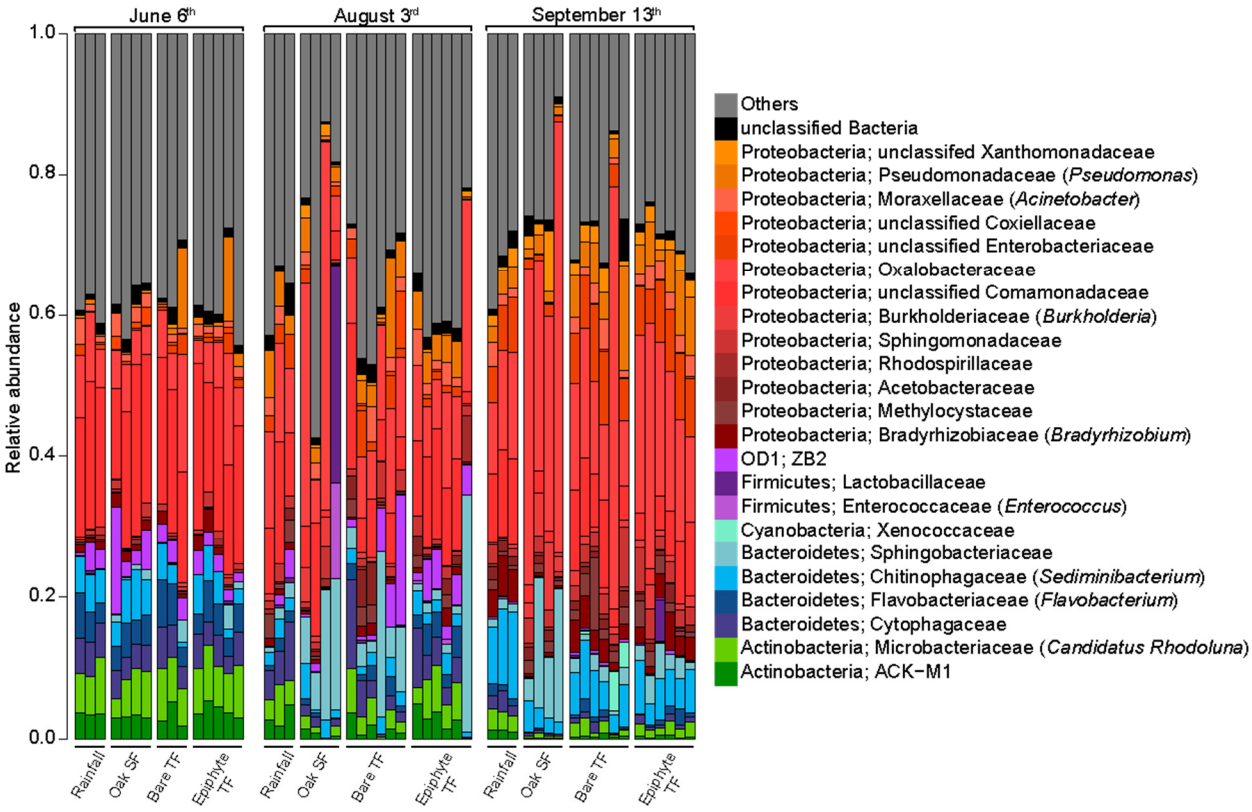

Figure 8. Distribution of bacterial taxa across samples in representative storm events. Relative abundances of taxa shown at family level. Taxa representing <5% of any population in any sample have been binned into "other." Stemflow denoted as SF and throughfall as TF.

6.2. Comparison of bacterial community composition across net rainfall fluxes

Hypothesis 2 is that bacterial community composition will differ significantly between rainfall, TF and SF. Hypothesis 3b is that bacterial community composition will significantly differ between bare canopy- and epiphyte-derived TF. Results testing Hypotheses 2 and 3b include visualization via non-metric multidimensional scaling (NMDS) analysis and statistical comparisons among samples' Bray-Curtis dissimilarity and Shannon's diversity indices (using descriptive statistics alongside PERMANOVA). Table 7 has been provided for the denotation of storm numbers to match calendar dates described previously and to provide the NOAA HYSPLIT model results depicting 48-h back-trajectories.

Table 7: Storm number and backtracking information from NOAA HYSPLIT model (Output for each storm in Appendix A). Storm dates in Table 4.

Storm Number	Origin	Prevailing Direction	Distance N-S	Distance E-W
14	NE Caribbean	S	-9°	-7°
16	NW Caribbean	SW	-12°	2°
17	Central Caribbean	S	-14°	-8°
18	Iowa/Missouri	NW	+8°	18°
19	N Gulf of Mex	W	-3°	6°
20	SW Florida	S	-5°	-1°
21	S Alabama	W	-1°	5°
22	W Sargasso Sea	E	3°	-7°
24	Central FL to Central Caribbean	NW	-8°	-2°
25	SW Sargasso Sea	E	-5°	-10°

Analysis of similarity among bacterial community composition between storms was visualized using NMDS, where proximity of samples within a 2-dimensional data reduction space indicates similarity (Figure 9). For an NMDS plot representing all samples, the stress value (0.161: Figure 9), which indicates the level of disagreement between the 2-D reduction space and

the observed community structures, is below the 0.2 threshold typically indicative of good representation in the selected space. Wide spacing between bacterial communities from the same canopy-derived hydrologic flux (rainfall, TF, or SF) suggests low similarity within sample types, including presence/absence of epiphyte cover (Figure 9). Again, this visualization indicates that the flow path rainfall takes through the phyllosphere to the pedosphere (SF versus SF) does not influence the composition of bacteria transported (rejection of Hypotheses 2 and 3b). Some fine-scale clusters in the NMDS plot are apparent, but are composed of individual events with the rain communities at the center individual event clusters, for example: storm 18 and, to a lesser extent, storm 17. Coarse scale clustering is observable in the NMDS plot, with several storms in the positive domain of axis 1 and negative domain of axis 2: storms 20-22 (Figure 9). These storms tend to have a common back-trajectory that begins over tropical maritime moisture sources, like the Sargasso Sea, storm 22, or near the Gulf of Mexico, storm 20 (Table 7). Interestingly, the storm 18 cluster is not only widely spaced away from the multi-storm 20-22 cluster (Figure 9), it has a very different back-trajectory, beginning over 20° latitude west (in the midwestern US) from the tropically-sourced events in the multi-storm cluster (Table 7). As storms cross clockwise into the opposite quadrant of where storm 18 plots, the back-trajectory origins move eastward (Figure 9; Table 7). In fact, the back-trajectory origin of storm 14 is 25° latitude to the east of storm 18 (Figure 9). Although north versus south varied as widely as east versus west in the storms‘ back-trajectory origins, the north-to-south differences in did not separate strongly in the NMDS plot (Figure 9). Interstorm variability in rainfall, TF and SF bacterial community composition appears to be driven by individual storm‘s source region and trajectory.

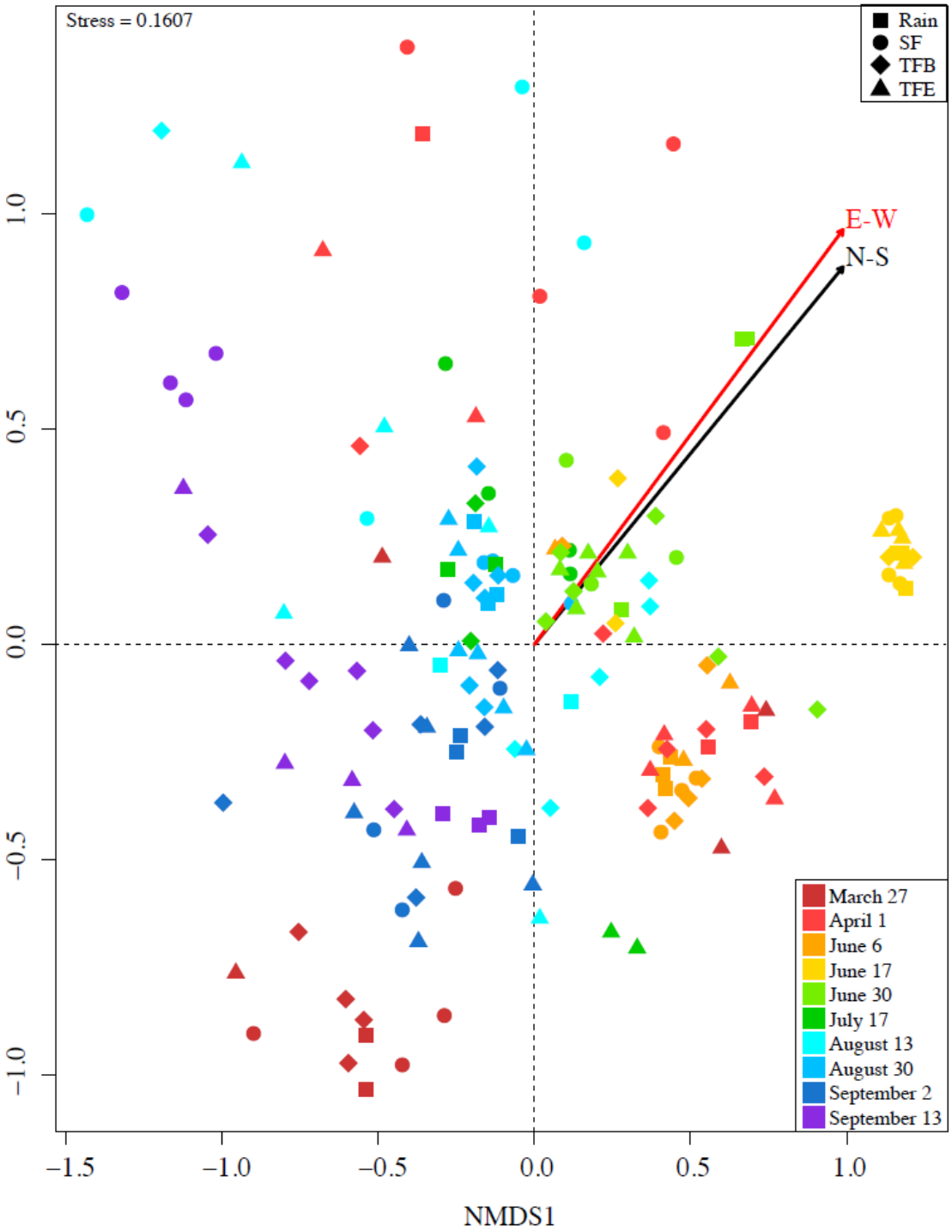

Figure 9. NMDS comparisons for all sample types, describing the relationship between storm samples and HYSPLIT back-trajectories (see Table 7).

6.3. Diversity and dissimilarity of bacterial communities in net rainfall fluxes

Visualization of sample dissimilarity via NMDS was confirmed using descriptive statistics and PERMANOVA (Bray-Curtis and Shannon's indices) for testing of Hypotheses 2 and 3b. Samples across 10 storms widely varied in bacterial species richness, from 2.5 to 6.2 (Figure 10a). However, within most individual storms, bacterial species richness was relatively similar among SF, bare TF, and epiphyte TF hydrologic fluxes (Figure 10a). Storms where similarities in bacterial species richness values are especially strong include storms 17 (4.5-5.5), 18 (~6), and 22 (3.75-4.75) (Figure 10a). Even when variability of bacterial species richness across hydrological fluxes within an individual storm is high (i.e., storm 21), the range of bacterial species richness is large and overlapping among net rainfall fluxes: 2.5-5.3 for SF versus 3.4-5.2 for TF (Figure 10a). Dissimilarity, whether weighted or unweighted, had similar medians, interquartile ranges, non-outlier ranges, and even lower-level outliers across fluxes and flux comparisons (Figures 10b-c). Thus, no trends in dissimilarity were observed in net rainfall flux comparisons. For example, median Bray-Curtis weighted and unweighted dissimilarity between flux types narrowly varied between 0.7-0.8 and 0.80-0.85, respectively (Figure 10b-c). Despite a narrow range in median weighted dissimilarity values across fluxes, the non-outlier range covered nearly the entire range of possible values (Figure 10b). Comparisons of SF bacterial community dissimilarity across storms and across other net rainfall fluxes yielded the greatest number of outliers (Figure 10b-c), like as a result of its greatest variability in species richness (Figure 10a). These metrics were also not statistically different per the PERMANOVA ($F = 1.286$, $p > 0.05$). A lack of statistically significant differences in the species richness and dissimilarity among rainfall, TF and SF - combined with the NMDS visualizations - suggests the

pathway rainwater travels through the canopy to the surface does not determine the community structure of bacteria delivered to forest soils during storms. Hypotheses 2 and 3b are rejected.

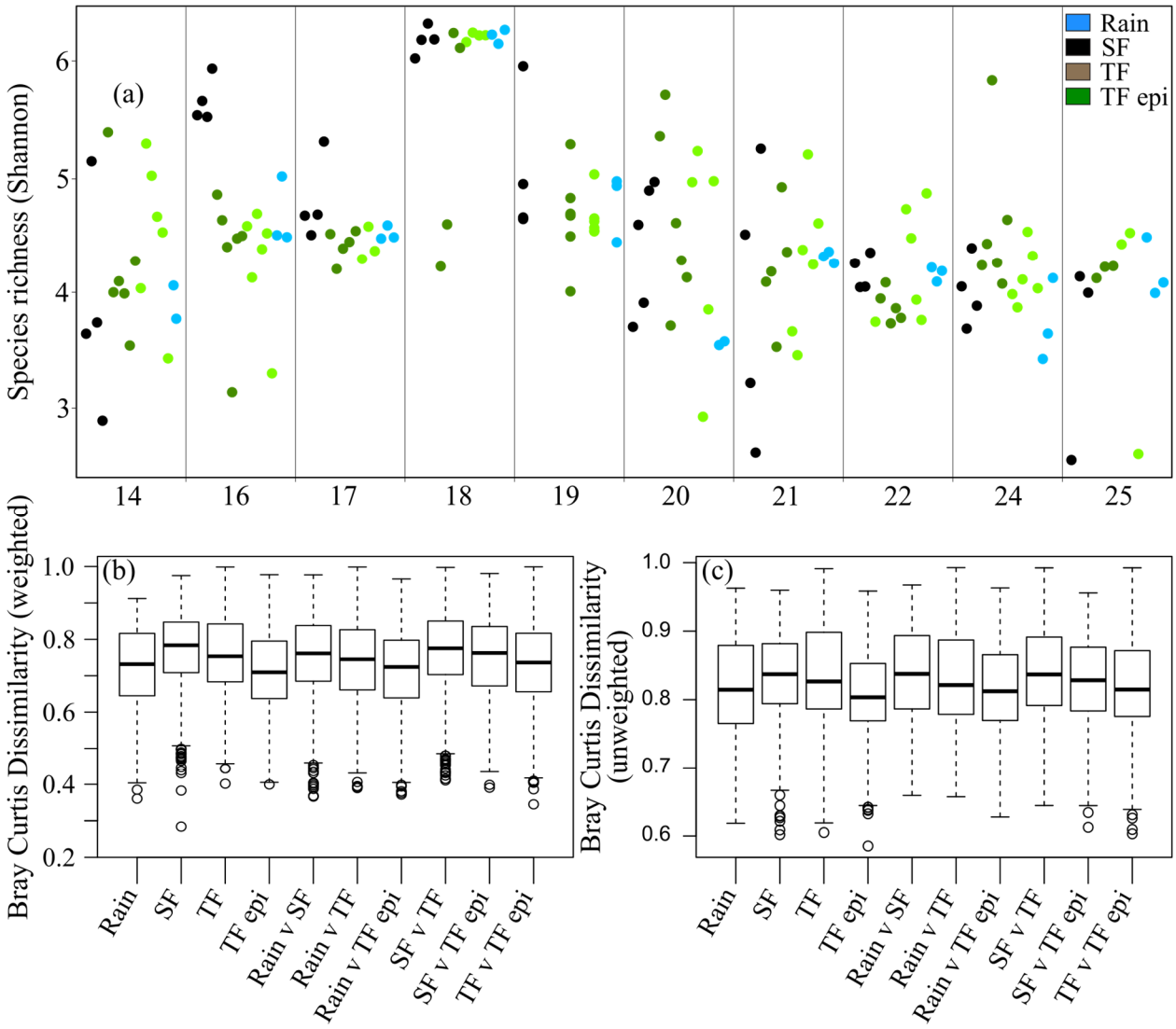

Figure 10. Bacterial community (a) species richness per Shannon's index and (b) dissimilarity per Bray-Curtis metric weighted and (c) unweighted for storm sample types.

6.4. Inter-storm diversity and dissimilarity of net rainfall bacterial communities

In contrast to similarity of bacterial community structure among rainfall, SF and TF, significant differences were observed in net rainfall bacterial community composition between storms (Figure 11). Median species richness ranged from 0.4-0.8 (Figure 11a). The storm with the greatest diversity and smallest weighted dissimilarity among samples was 17-Jun-2016 (Figure 11a-b), which was the fastest-moving storm system—indicated by the furthest away NOAA HYSPLIT back-trajectory (Table 7). All source areas for the 17-Jun-2016 storm were also over homogenous midwestern continental land (Table 7). On the other hand, storms with the largest ranges in species richness and some of the highest median dissimilarity values (1-Apr-2016 and 3-Aug-2016: Figures 11b-c) were slow (48 h back-trajectories originated from nearby) and composed of air masses from coastlines areas with land and ocean surfaces (Table 7). Species richness and dissimilarity in bacterial communities were statistically distinct between groups of storms that differed in source area (PERMANOVA: $F = 7.476$, $p < 0.001$). Thus, it appears storm back-trajectories may control bacterial community composition in rain, TF, and SF.

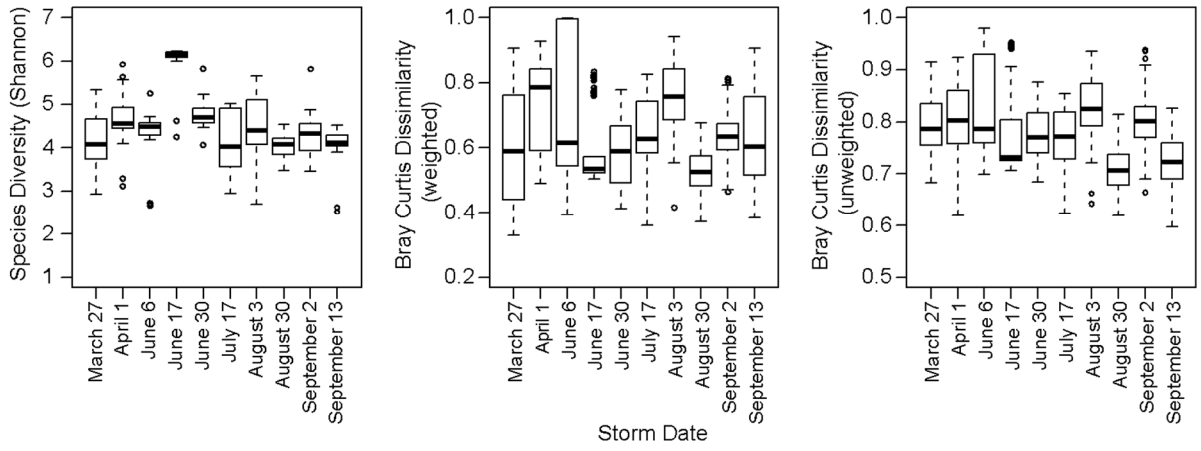

Figure 11. Shannon's diversity index and Bray-Curtis dissimilarity measurements for individual storms.

CHAPTER 7

DISCUSSION

7.1. Net rainfall dynamics of epiphyte-laden Quercus virginiana

Accomplishment of **Objective 0** found that, for *Q. virginiana*, SF water flux (Figure 7) was generally one-third lower than that of oak TF (Figure 6). These values agree well with those from the literature on similar species (Levia et al., 2011). As the study species is evergreen and rainfall is evenly distributed throughout the year (Figure 3), there were no clear seasonal patterns in TF or SF water fluxes (data not shown, but described in Van Stan et al. (2017)). Rather, variability in these canopy-derived hydrologic fluxes was overwhelmingly driven by storm magnitude (mm) (Figures 6-7). Previous studies have found that intra-seasonal variability in TF and SF water fluxes are significantly and linearly related to storm size (Eaton et al., 1973; Zhang et al., 2015), with canopy structure driving the steepness of the slope (Park and Cameron, 2008; Sadeghi et al., 2016). Rainfall for the study site measured 1278 mm for 2015 and 1074 mm for 2014, which has similar rainfall amounts for the studies summarized in the Llorens & Domingo (2007) review paper of Mediterranean forests (of which there are many oaks).

7.2. Bacterial concentration and flux from forests during rainfall

Hypotheses 1a-c were supported by my results. *Quercus virginiana* had bacterial concentrations significantly greater than for open rainfall, showing that the bacterial biomass detected in this study originated from tree surfaces saturated and washed by rainfall. There was

no linear relationship between bacterial concentrations and any storm conditions. Median bacterial cell concentration was greater for SF than TF (Hypothesis 1a; Table 6). These results also showed that SF is a significant source of cells to a localized area of the forest floor. SF's substantial bacterial concentrations are likely because this flow (1) has extensive contact with bark surfaces where microbial life is more sheltered, permitting large and diverse bacterial populations to thrive (Stone et al., 2000; Anderson, 2014) and (2) scours these rough surfaces with more rainwater relative to TF. However, extra epiphyte cover did not significantly increase bacterial cell concentrations, rejecting **Hypothesis 3a**.

Enrichment at, and exceeding, levels observed for bacterial concentrations in this study has been commonly reported for TF and SF solutes (Heartsill-Scalley et al., 2007; Zhang et al., 2016; Schooling et al., 2017). Intracellular fluids in bacteria are highly enriched in solutes (Brown, 1964) that SF and TF studies have often attributed to leaching from foliar surfaces (i.e, K^+) and dry deposition (i.e., Na^+ and Cl^- from sea salt aerosols) (Staelens et al., 2007; André et al., 2008; Van Stan et al., 2012). The assumption of negligible Na^+ and Cl^- leaching from forest canopies, in particular, has been eroded by recent work (i.e., Thimonier et al., 2011; Montelius et al., 2015). However, no mechanisms explaining how these solutes enter TF and SF from plant tissues has been proposed. Cell lysis of even a portion of the millions of bacteria scoured from the phyllosphere during a rain event may represent a mechanism explaining sources of solutes (like Na+ and Cl-) to TF and SF previously attributed solely to atmospheric aerosols and/or plant tissue leaching.

Since TF from the canopies dominated the areal proportion of sub-canopy rainfall flux at this site, TF produced the greatest annual flux (Hypothesis 1b: Table 6). TF fluxes frequently

exceeded 5 E+8 bacteria m^{-2} mm^{-1} of rainfall, with generally less variability than SF. SF produced the largest median bacterial fluxes per m^2 of infiltration area for both species, followed by TF, then rainfall, whether normalized by storm duration (cells m^{-2} h^{-1}, Figure 8b) or intensity (cells m^{-2} mm^{-1}, Figure 8c). SF fluxes scaled as cells ha^{-1} $year^{-1}$ often appear insignificant, as even the annual bacterial flux of "free" TF (i.e., rainfall that passes through gaps in the canopy) was double the sum of SF flux (Table 5). However, substantial, highly-localized SF fluxes to the trunk base can preferentially travel through soils along root macropores, bathing the rhizosphere (Johnson and Lehmann, 2006; Johnson and Jost, 2011). The highly concentrated nature of SF was found to alter soil microbial community structure around trunks (Rosier et al., 2016). The generally >1 E+9 bacteria m^{-2} h^{-1} flux to oak and soils during storms may have a role in contributing community members to the near-stem soils and rhizosphere, directly (as member of the active soil communities) or indirectly (as a source of intracellular organic and inorganic matter to the resident soil communities).

Annual net rainfall bacterial flux greatly exceeded gross rainfall bacterial flux (Hypothesis 1c: Table 6). It is important to note that these are "free" bacteria and do not include particle-attached bacteria, so this the annual net rainfall bacterial flux is probably larger. Given that a single *E. coli* cell weighs ~1 E-15 kg, this value equates to ~2 kg of bacterial cells fluxed to soils each year by TF and SF for an epiphyte-laden oak forest with substantial rainfall interception (Van Stan et al., 2016). Where the vegetation canopy is structured to increase TF or SF, for example, in beech (*Fagus* spp.) forests (Staelens et al., 2008) or shrublands (Li et al., 2008), bacterial fluxes from the vegetation to the forest floor during rainfall may be greater. Thus, data on concentration, flux, and community structure/function of suspended bacteria are

needed for TF and SF from diversely vegetated sites. If these cells are viable, trees may be introducing beneficial or pathogenic microbes into their soils and, in the case of SF or TF drip points, their rhizospheres. Residence time of water routed through the phyllosphere affects the spread of foliar pathogens (Garbelotto et al., 2003), so canopy-derived hydrologic fluxes may also provide a pathway of infection for pathogens through the soil.

If lysed, TF and SF may be contributing a large subsidy of highly biolabile solutes and organic matter from intracellular materials to soils that could prime soil organic matter transformation (Kuzyakov, 2010) or initiate microbial hot spots/moments (Kuzyakov and Blagodatskaya, 2015). For example, the annual bacterial cell count from this study, when lysed, could represent nearly 2 kg ha^{-1} $year^{-1}$ of carbon inputs (Fagerbakke et al., 1996), of which 0.2-1.3 kg ha^{-1} $year^{-1}$ could be from cellular proteins (Zubkov et al., 1999). Whether active or lysed once in the soil, phyllosphere bacterial communities carried by TF and SF are likely to play important biogeochemical roles in the forest surface. Thus, the bacterial flux identified in this study is a missing key component of (1) canopy biogeochemical budgets, (2) litter and soil microbial ecology, and (3) the mechanistic understanding of biosphere-atmosphere interactions and matter transport. Unfortunately, the sources of the solutes are not observed in TF and SF chemistry (i.e., Cl^- per Thimonier et al., 2008). A possibility for this discrepancy may be due to lysis of bacterial cells, with degrading cellular structures providing nutrients.

7.3. Composition of bacterial communities in TF and SF

Hpotheses 2 and 3b were rejected as results indicate that the bacterial community composition of TF and SF is strongly tied to atmospherically-transported bacteria (Figures 8-11). The path rainwater travels through the phyllosphere appears to have a minor effect on the bacterial taxa delivered to the pedosphere during storms (Figures 9-10). This is an unexpected result because (i) previous work found that the dermosphere (bark surface) and phyllosphere select for distinct bacterial communities (Lambais et al. 2014), and (ii) SF and TF primarily flow along bark and leaves, respectively. These findings are also counterintuitive to previous findings at the same site; specifically, TF and SF bacterial concentrations are significantly greater than in rain, 10.4E+5 cells mL^{-1} versus 0.5E+5 cells mL^{-1} (Pound et al. 2017). It is seemingly paradoxical that rainwater entrained as TF and SF in the canopy becomes enriched in the same bacterial taxa carried by the rainwater itself. However, aerosolized bacteria that become cloud condensation nuclei (Bauer et al. 2003), and eventually rain, are constantly deposited onto terrestrial surfaces during the dry period between storms (Tong and Lighthart 2000). The ostensible paradox is, thus, resolved if the rainwater entrained in TF and SF is being enriched with similar bacterial taxa that were atmospherically deposited onto the canopy prior to the storm. This raises questions regarding the dynamics of the phyllosphere bacterial community. For instance, are there two community factions in the phyllosphere that experience different disturbance regimes: a weakly-attached atmospherically deposited and strongly-attached phyllosphere bacterial community? Do the similar protective strategies observed in soils and streams (i.e., biofilms), thus, only protect specific factions of the bacterial community on canopy surfaces from being scoured away by rainwater?

The bacterial taxa identified in TF and SF are found as aerosols that catalyse ice formation, cloud growth and subsequent "bioprecipitation," as well as on the phyllosphere. In particular, Proteobacteria (the most abundant phylum in our net rainfall fluxes: Figure 8) are abundant community members in the phyllosphere (Vorholt 2012) and in aerosols (Radosevich et al. 2002). The abundance of specific families within the Proteobacteria phylum indicate aerosolized bacteria are a significant source for TF and SF. For example, Pseudomonas represents one of the most common aerosols above plant canopies and is a common ice nucleation-active family responsible for initiating cloud microphysical processes that lead to bioprecipitation (Morris et al. 2013). Many other Proteobacteria families (Xanthomodaceae, Moraxellaceae, Enterobacteriaceae, etc.) are considered primary biological aerosols and have been found to be abundant downwind from urban environments (Després et al. 2012)—like Savannah (Georgia, USA) near our site. The presence of Firmicutes and Cyanobacteria further indicate an aerosolized bacterial source to TF and SF, as these phyla contribute to primary biological aerosols (Després et al. 2012) but are not found or represent so small a portion of the forest phyllosphere and dermosphere bacterial communities (Redford et al. 2010; Kim et al. 2012; Lambais et al. 2014) that they are not even mentioned in review works focused on phyllosphere microbial communities (Vorholt 2012). Atmospheric transport of Acidobacteria to the tree canopy is also plausible as these have been observed in cloud water (Kourtev et al. 2011) and hailstones (Šantl-Temkiv et al. 2013); however, this phylum (and Actinobacteria) can be abundant on forest canopy surfaces (Kim et al. 2012). Considering the importance of atmospheric transport and deposition processes in TF and SF bacterial community structure, perhaps the interspecific differences in phyllosphere, dermosphere, and epiphyte bacterial

communities (Brighigna et al. 1999; Fürnkranz et al. 2008; Lambais et al. 2104) aren't as critical as the large-scale storm synoptic patterns (Siegert et al. 2017).

Previous work at this site finds that TF and especially SF supply a rapid and substantial enough bacterial flux during storms, ~30 billion cells m^{-2} h^{-1}, to potentially inoculate soils (Pound et al. 2017). Should TF and SF bacteria be able to access or establish communities at the forest floor, there may be broad biogeochemical implications for the litter layer and topsoil. The most abundant phylum in net rainfall fluxes, Proteobacteria, plays many key roles in the cycling of carbon, sulfur and nitrogen as a result of their diversity in energy-generating mechanisms (Kersters et al. 2006). Some examples include (i) diazotrophic bacteria in Oxalobacteriaceae that fix atmospheric nitrogen, (ii) genera of Sphingomonadaceae that can metabolize aromatic carbon compounds, and (iii) sulfur-oxidizing Enterobacteriaceae and Pseudomonadaceae species (Kersters et al. 2006). Proteobacteria also contain some of the most prominent genera in litter decomposition (Aneja et al. 2006), although Actinobacteria and Bacteroidetes (including genera identified in TF and SF) have been found to be abundant throughout litter decomposition as well (Tláskal et al. 2016). Hot moments of bacterial transport to soil substrates, like observed for TF and SF (Pound et al. 2017), are relevant to soil biogeochemical cycling for branch- and filament-forming microbes like Cyanobacteria (Kuzyakov and Blagodatskaya 2015). Although less abundant in TF and SF, Acidobacteria are versatile heterotrophs capable of metabolizing a large range of organic carbon compounds (sugars, cellulose, chitin, etc.), nitrate and nitrite reduction, forming biofilms, stabilizing soil structures, and producing antimicrobial compounds in soils (Ward et al. 2009). Therefore, future work is merited regarding the fate/potential influence of TF and SF bacterial communities at the forest floor.

CHAPTER 8

CONCLUSIONS AND FUTURE DIRECTIONS

Rainfall partitioning of the epiphyte-laden *Quercus virginiana* (southern live oak) canopy at Skidaway Island compared favorably to other oak studies around the globe – with SF being somewhat smaller (extra epiphyte water storage). Despite low SF generation, the bacterial concentration and flux as determined with flow cytometry was impressive (# cells m^{-2} $storm^{-1}$). Bacterial concentrations were found to be significantly different, increasing from rainfall < TF << SF. Thus, assuming bacterial fluxes from gross rainfall are representative of what reaches the forest floor is incorrect. In fact, open rainfall annual flux was 1.3 E+14 cells ha^{-1} y^{-1} versus the net rainfall annual flux of 15 E+15 cells ha^{-1} y^{-1}. This is clearly a large flux of bacteria that have yet to be accounted for, especially if these bacteria are alive and actively transforming nutrients in the soils around trees.

The bacterial community structure, surprisingly, did not differ between rainfall, SF and TF despite each flux interacting with different spheres (atmosphere – rainfall, leaves/epiphytes – TF, bark – SF). Diversity and dissimilarity of bacterial communities in net rainfall were also not affected by the presence of epiphytes. The epiphytes were likely preventing fluxes of bacterial communities found on their surface, as the bacteria may have formed biofilms or other fastidious holds along the plant tissues.

Many questions still remain from this work, I recommend future work on net rainfall interactions with microbial communities address the following questions:

- What is the amount and composition of the fungal community (especially conidia)

transported by TF and SF?

- This study focused on one species, but are there inter-specific differences in TF or SF microbial community composition?
- What proportion of cells being fluxed during storms are alive or dead?
- Can the bacteria in TF and SF access soil refugia (biofilms, etc) and become successfully integrated into the soil microbial community?
- Does SF contribute critical bacteria (N-fixing nodule formers) or fungi (mycorrhizae) to the rhizosphere?
- What are the dominant functional genes in TF and SF microbial communities? Moreover, what do these functional genes mean for processing nutrients in TF and SF during transport?
- Can we use mesoscale synoptic meteorological forecasting to accurately predict the bacterial and fungal community composition and flux in TF and SF?

The work toward addressing fungal conidial transport and composition in TF and SF has begun (Gönczöl and Révay, 2004; Magyar and Révay, 2009; Sridhar et al., 2006; Magyar 2008). But, major studies to determine the communities of fungi present in TF and SF have not been sufficiently completed. The study site at Skidaway is also currently collecting data on *Juniperus virginiana*, and would make a sufficient site for studying the inter-specific differences in TF and SF microbial community composition. The different nutrients leached from the tree species may affect soil communities, which has not been compared. Bacteria being deposited to the forest floor during rainfall events are dynamic, and may or may not cause cellular deaths during the process. The cell's viability can be determined using flow cytometry with a live/dead indicator kit. This can determine whether the bacteria will contribute to nutrient cycling once deposited in

the soil or will deposit nutrients once the cells lyse.

The bacteria in TF and SF may or may not be able to form biofilms among plant or soil surfaces, which can increase survival rate during times of nutrient scarcity. Again, the viability of cells would need to be established and a study performed on the inoculating effect of bacteria during storms. Of the bacteria capable of creating biofilms, other bacteria may be able to form nodules with plants, or fungi to form mycorrhyzal relationships with plants. This can be tested in a greenhouse study with bacteria being inoculated into soil conditions similar to the study site and observing nitrogen transformation among the root systems of plants (Rosier et al., 2015).

For functional gene analysis, novel software such as PICRUSt can compare sequences of bacteria to databases to determine what roles the species will play in the soil once inoculated. Other methods such as denaturing gradient gel electrophoresis can be performed to determine similar results. We assume what we see in TF and SF chemistry is from (1) leaching of tree tissues and (2) atmospheric deposition (DD). Maybe functional genes are distorting the picture and these fluxes are not useful to infer leaching and DD.

Storm backtracking has shown that bacterial communities can be affected by the origin point and patterns of storms, further observation of storms and comparisons of community structure will allow more accurate assessments of the role of storm processes effect on the aerosolized microbial community structure.

REFERENCES

Abdelli, F., 1999. Analisis comparative de la contribucion de distintas comunidades vegetales a la distribucion del agua de Lluvia, a la conservacion delag ua en el suelo y a la recarga de acuiferos en medios semiaridos. Masters Thesis, CIHEAM, Zaragoza, 177 pp.

Alewell, C. (2001). Predicting reversibility of acidification: the European sulfur story. *Water, Air, and Soil Pollution*, *130*(1-4), 1271-1276.

Andersson, T. (1991). Influence of stemflow and throughfall from common oak (Quercus robur) on soil chemistry and vegetation patterns. Canadian Journal of Forest Research, 21(6), 917-924.

Andrews, J. H., & Harris, R. F. (2000). The ecology and biogeography of microorganisms on plant surfaces. *Annual review of phytopathology*, *38*(1), 145-180.

Asplund, J., & Wardle, D. A. (2014). Within-species variability is the main driver of community-level responses of traits of epiphytes across a long-term chronosequence. *Functional ecology*, *28*(6), 1513-1522.

Avila, A., & Rodrigo, A. (2004). Trace metal fluxes in bulk deposition, throughfall and stemflow at two evergreen oak stands in NE Spain subject to different exposure to the industrial environment. *Atmospheric Environment*, *38*(2), 171-180.

Avila, A., & Rodrigo, A. (2004). Trace metal fluxes in bulk deposition, throughfall and stemflow at two evergreen oak stands in NE Spain subject to different exposure to the industrial environment. Atmospheric Environment, 38(2), 171-180.

Backnäs, S., Laine-Kaulio, H., & Kløve, B. (2012). Phosphorus forms and related soil chemistry in preferential flowpaths and the soil matrix of a forested podzolic till soil profile. Geoderma, 189, 50-64.

Berger, T. W., Eagar, C., Likens, G. E., & Stingeder, G. (2001). Effects of calcium and aluminum chloride additions on foliar and throughfall chemistry in sugar maples. Forest Ecology and Management, 149(1), 75-90.

Bischoff, S., Schwarz, M. T., Siemens, J., Thieme, L., Wilcke, W., & Michalzik, B. (2015). Properties of dissolved and total organic matter in throughfall, stemflow and forest floor leachate of central European forests.*Biogeosciences*, *12*(9), 2695-2706.

Boxman, R. L., Parkansky, N., Mamane, H., Meirovitz, M., Orkabi, Y., Halperin, T., ... & Cheskis, S. (2008). Pulsed Submerged Arc Plasma Disinfection of Water: Bacteriological Results and an Exploration of Possible Mechanisms. In *Plasma Assisted Decontamination of Biological and Chemical Agents* (pp. 41-50). Springer, Dordrecht.

Brighigna et al. (2000) The influence of air pollution on the phyllosphere microflora composition of *Tillandsia* leaves (Bromeliaceae). Rev Biol Trop, 48, http://www.scielo.sa.cr/scielo.php?pid=S0034-77442000000200024&script=sci_arttext&tlng=pt

Brighigna et al. (1992) Role of nitrogen-fixing bacterial microflora in the epiphytism of *Tillandsia* (Bromeliaceae). Am J Bot, 79, 723-727.

Bringel, F., & Couée, I. (2015). Pivotal roles of phyllosphere microorganisms at the interface between plant functioning and atmospheric trace gas dynamics. Frontiers in microbiology, 6, 486.

Brockett, B. F. T., Prescott, C. E., & Grayston, S. J. (2012). Soil moisture is the major factor influencing microbial community structure and enzyme activities across seven biogeoclimatic zones in western canada. Soil Biology and Biochemistry, 44(1), 9-20.

Burrows, S. M., Butler, T., Jöckel, P., Tost, H., Kerkweg, A., Pöschl, U., & Lawrence, M. G. (2009). Bacteria in the global atmosphere–Part 2: Modeling of emissions and transport between different ecosystems. *Atmospheric Chemistry and Physics*, *9*(23), 9281-9297.

Carlisle, A. L., Brown, A. H. F., & White, E. J. (1967). The organic matter and nutrient elements in the precipitation beneath a sessile oak (Quercus petraea) canopy. The Journal of Ecology, 87-98.

Carlyle-Moses, D. E. (2004). Throughfall, stemflow, and canopy interception loss fluxes in a semi-arid Sierra Madre Oriental matorral community. Journal of Arid Environments, 58(2), 181-202.

Carlyle-Moses, D. E., & Gash, J. H. (2011). Rainfall interception loss by forest canopies. In Forest Hydrology and Biogeochemistry (pp. 407-423). Springer Netherlands.

Carroll, G. C. (1980). Forest canopies: complex and independent subsystems. *Forests: fresh perspectives from ecosystem analysis. Oregon State University Press, Corvallis*, 87-108.

Ceccherini, M. T., Ascher, J., Agnelli, A., Certini, G., Pietramellara, G., Piovanelli, C., & Nannipieri, P. (2008). Tree bark and soil ammonia oxidizers: a molecular study on a historical forest of central Italy. Fresenius Environmental Bulletin, 17(7 B), 882-889.

Chang, S. C., & Matzner, E. (2000). The effect of beech stemflow on spatial patterns of soil solution chemistry and seepage fluxes in a mixed beech/oak stand. Hydrological Processes, 14(1), 135-144.

De Schrijver, A., Nachtergale, L., Staelens, J., Luyssaert, S., & De Keersmaeker, L. (2004). Comparison of throughfall and soil solution chemistry between a high-density Corsican pine stand and a naturally regenerated silver birch stand. *Environmental Pollution*, *131*(1), 93-105.

DeSantis et al., (2006). Greengenes, a chimera-checked 16S rRNA gene database and workbench compatible with ARB. *Applied and Environmental Microbiology*, *72*, 5069-5072.

Eaton, J. S., Likens, G. E., & Bormann, F. H. (1973). Throughfall and stemflow chemistry in a northern hardwood forest. The Journal of Ecology, 495-508.

Eaton, J. S., Likens, G. E., & Bormann, F. H. (1978). The input of gaseous and particulate sulfur to a forest ecosystem. *Tellus*, *30*(6), 546-551.

Edgar, R. C., Haas, B. J., Clemente, J. C., Quince, C., & Knight, R. (2011). UCHIME improves sensitivity and speed of chimera detection. *Bioinformatics*, 27(16), 2194-2200.

Endo, I., Ohte, N., Iseda, K., Tanoi, K., Hirose, A., Kobayashi, N. I., ... & Ohashi, M. (2015). Estimation of radioactive 137-cesium transportation by litterfall, stemflow and throughfall in the forests of Fukushima. *Journal of environmental radioactivity*, *149*, 176-185.

Evans, C. A., Coombes, P. J., & Dunstan, R. H. (2006). Wind, rain and bacteria: the effect of weather on the microbial composition of roof-harvested rainwater. Water research, 40(1), 37-44.

Fathizadeh, O., Attarod, P., Pypker, T. G., Darvishsefat, A. A., & Amiri, G. Z. Seasonal Variability of Rainfall Interception and Canopy Storage Capacity Measured under Individual Oak (Quercus brantii) Trees in Western Iran.

Finkel, O. M., Burch, A. Y., Lindow, S. E., Post, A. F., & Belkin, S. (2011). Geographical location determines the population structure in phyllosphere microbial communities of a salt-excreting desert tree. *Applied and environmental microbiology*, *77*(21), 7647-7655.

Fürnkranz et al. (2008) Nitrogen fixation by the phyllosphere bacteria associated with higher plants and their colonizing epiphytes of a tropical lowland rainforest of Costa Rica. ISME J, 2, 561-570.

Garth, R. E. (1964). The ecology of Spanish moss (Tillandsia usneoides): its growth and distribution. *Ecology*, *45*(3), 470-481.

Gönczöl, J., & Révay, Á. (2003). Treehole fungal communities: aquatic, aero-aquatic and dematiaceous hyphomycetes. *Fungal Diversity*, *12*, 19-34.

Gosz, J. R., Likens, G. E., & Bormann, F. H. (1976). Organic matter and nutrient dynamics of the forest and forest floor in the Hubbard Brook Forest.*Oecologia*, *22*(4), 305-320.

Hauck, M., Paul, A., Gross, S., & Raubuch, M. (2003). Manganese toxicity in epiphytic lichens: chlorophyll degradation and interaction with iron and phosphorus. *Environmental and Experimental Botany*, *49*(2), 181-191.

Henderson, G. S., Harris, W. F., Todd Jr, D. E., & Grizzard, T. (1977). Quantity and chemistry of throughfall as influenced by forest-type and season. The Journal of Ecology, 365-374.

Hinton, M.J., S.L. Schiff, and M.C. English (1997), The significance of storms for the concentration and export of dissolved organic carbon from two Precambrian Shield catchments. *Biogeochem., 36,* 67-88.

Hirano, S. S., & Upper, C. D. (2000). Bacteria in the Leaf Ecosystem with Emphasis on Pseudomonas syringae—a Pathogen, Ice Nucleus, and Epiphyte. *Microbiology and molecular biology reviews*, *64*(3), 624-653.

Hogan, L. A. (2012). Oak. https://web.archive.org/web/20130523173442/http://www.eoearth.org/article/Oak

Hölscher, D., Köhler, L., van Dijk, A. I., & Bruijnzeel, L. S. (2004). The importance of epiphytes to total rainfall interception by a tropical montane rain forest in Costa Rica. *Journal of Hydrology*, *292*(1), 308-322.

Ivens, W., Kauppi, P., Alcamo, J., & Posch, M. (1990). Sulfur deposition onto European forests: throughfall data and model estimates. *Tellus B*, *42*(3), 294-303.

Keim, R.F., and A.E. Skaugset (2004), A linear system model of dynamic throughfall rates beneath forest canopies. Water Resour. Res., 40, W05208.

Kourtev, P. S., Hill, K. A., Shepson, P. B., & Konopka, A. (2011). Atmospheric cloud water contains a diverse bacterial community. *Atmospheric environment*, *45*(30), 5399-5405.

Kozich JJ, Westcott SL, Baxter NT, Highlander SK, Schloss PD. (2013): Development of a dual-index sequencing strategy and curation pipeline for analyzing amplicon sequence data on the MiSeq Illumina sequencing platform. Applied and Environmental Microbiology. 79(17):5112-20.

Kristensen, H. L., Gundersen, P., Callesen, I., & Reinds, G. J. (2004). Throughfall nitrogen deposition has different impacts on soil solution nitrate concentration in European coniferous and deciduous forests. Ecosystems, 7(2), 180-192.

Lambais, M. R., Crowley, D. E., Cury, J. C., Büll, R. C., & Rodrigues, R. R. (2006). Bacterial diversity in tree canopies of the Atlantic forest. Science, 312(5782), 1917-1917.

Lamersdorf, N. P., & Blank, K. (1995). Evaluation of fine material input with throughfall for a spruce forest in Solling, FRG, by means of a roof construction. Ecosystem Manipulation Experiments: Scientific Approaches, Experimental Design and Relevant Results, edited by: Jenkings, A., Ferrier, R., and Kirby, C, (23), 168-170.

Lee, E.J., N. Kenkel, and T. Booth (1996), Atmospheric deposition of macronutrients by pollen in the boreal forest. *Ecoscience*, *3,* 304-309.

Leininger, T. D., & Winner, W. E. (1988). Throughfall chemistry beneath Quercus rubra: atmospheric, foliar, and soil chemistry considerations.*Canadian Journal of Forest Research*, *18*(4), 478-482.

Le Mellec, A., & Michalzik, B. (2008). Impact of a pine lappet (Dendrolimus pini) mass outbreak on C and N fluxes to the forest floor and soil microbial properties in a Scots pine forest in Germany. Canadian Journal of Forest Research, 38(7), 1829-1841.

Le Mellec, A., Meesenburg, H., & Michalzik, B. (2010). The importance of canopy-derived dissolved and particulate organic matter (DOM and POM)–comparing throughfall solutionfrom broadleaved and coniferous forests.*Annals of Forest Science*, *67*(4), 411.

Le Mellec, A., Meesenburg, H., & Michalzik, B. (2010). The importance of canopy-derived dissolved and particulate organic matter (DOM and POM)–comparing throughfall solutionfrom broadleaved and coniferous forests. Annals of Forest Science, 67(4), 411.

Lequy, E., Calvaruso, C., Conil, S., & Turpault, M. P. (2014). Atmospheric particulate deposition in temperate deciduous forest ecosystems: Interactions with the canopy and nutrient inputs in two beech stands of Northeastern France. *Science of the Total Environment*, *487*, 206-215.

Leveau, J. H., & Lindow, S. E. (2001). Appetite of an epiphyte: quantitative monitoring of bacterial sugar consumption in the phyllosphere. *Proceedings of the National Academy of Sciences*, *98*(6), 3446-3453.

Levia Jr, D. F., & Frost, E. E. (2006). Variability of throughfall volume and solute inputs in wooded ecosystems. Progress in Physical Geography, 30(5), 605-632.

Li, X. Y., Yang, Z. P., Li, Y. T., & Lin, H. (2009). Connecting ecohydrology and hydropedology in desert shrubs: stemflow as a source of preferential flow in soils. *Hydrology and Earth System Sciences*, *13*(7), 1133.

Lindow, S. E., & Brandl, M. T. (2003). Microbiology of the phyllosphere. Applied and environmental microbiology, 69(4), 1875-1883.

Llorens, P., & Domingo, F. (2007). Rainfall partitioning by vegetation under Mediterranean conditions. A review of studies in Europe. *Journal of Hydrology*, *335*(1), 37-54.

MacKinnon, J. A. (1982). Stemflow and throughfall mycobiota of a trembling aspen-red alder forest (Doctoral dissertation, University of British Columbia).

Magyar, D. (2008). The tree bark: a natural spore trap. Asp Appl Biol, 89, 7-16.

Magyar, D., & Révay, Á. (2009). New species of Oncopodiella (Hyphomycetes) from living trees. Nova Hedwigia, 88(1-2), 169-182.

Mahowald, N., Jickells, T. D., Baker, A. R., Artaxo, P., Benitez-Nelson, C. R., Bergametti, G., ... & Kubilay, N. (2008). Global distribution of atmospheric phosphorus sources, concentrations and deposition rates, and anthropogenic impacts. *Global Biogeochemical Cycles*, *22*(4).

Manderscheid, B., & Matzner, E. (1995). Spatial and temporal variation of soil solution chemistry and ion fluxes through the soil in a mature Norway spruce (Picea abies (L.) Karst.) stand. Biogeochemistry, 30(2), 99-114.

Martin, C. E., & Schmitt, A. K. (1989). Unusual water relations in the CAM atmospheric epiphyte Tillandsia usneoides L.(Bromeliaceae). *Botanical Gazette*, *150*(1), 1-8.

McDonald, D., Price, M. N., Goodrich, J., Nawrocki, E. P., DeSantis, T. Z., Probst, A., ... & Hugenholtz, P. (2012). An improved Greengenes taxonomy with explicit ranks for ecological and evolutionary analyses of bacteria and archaea. *The ISME journal*, *6*(3), 610-618.

McDowell, W. H., & Likens, G. E. (1988). Origin, composition, and flux of dissolved organic carbon in the Hubbard Brook Valley. Ecological monographs, 58(3), 177-195.

Michalzik, B., & Stadler, B. (2005). Importance of canopy herbivores to dissolved and particulate organic matter fluxes to the forest floor. *Geoderma*,*127*(3), 227-236.

Moreno, G., Gallardo, J. F., & Bussotti, F. (2001). Canopy modification of atmospheric deposition in oligotrophic Quercus pyrenaica forests of an unpolluted region (central-western Spain). *Forest Ecology and Management*,*149*(1), 47-60.

Morris, C. E., & Kinkel, L. L. (2002). Phyllosphere microbiology. *eds. Lindow SE, Hecht-Poinar EI, and Elliot V, APS Press, St. Paul*, 365-375.

Muller, C. H., Hanawalt, R. B., & McPherson, J. K. (1968). Allelopathic control of herb growth in the fire cycle of California chaparral. *Bulletin of the Torrey Botanical Club*, 225-231.

Mużyło, A., Llorens, P., & Domingo, F. (2012). Rainfall partitioning in a deciduous forest plot in leafed and leafless periods. *Ecohydrology*, *5*(6), 759-767.

Nadkarni, N. M., & Sumera, M. M. (2004). Old-Growth Forest Canopy Structure and Its Relationship to Throughfall Interception. Forest Science, 50, 3.

Neff, J. C., & Asner, G. P. (2001). Dissolved organic carbon in terrestrial ecosystems: synthesis and a model. *Ecosystems*, *4*(1), 29-48.

Nemergut, D. R., Cleveland, C. C., Wieder, W. R., Washenberger, C. L., & Townsend, A. R. (2010). Plot-scale manipulations of organic matter inputs to soils correlate with shifts in microbial community composition in a lowland tropical rain forest. *Soil Biology and Biochemistry, 42*(12), 2153-2160.

Multivariate Analysis of Ecological Communities in R: vegan tutorial Jari Oksanen June 10, 2015 http://cc.oulu.fi/~jarioksa/opetus/metodi/vegantutor.pdf

Pereira, F. L., et al. "Modelling interception loss from evergreen oak Mediterranean savannas: Application of a tree-based modelling approach."*Agricultural and Forest Meteorology* 149.3 (2009): 680-688.

Pruesse, E., Quast, C., Knittel, K., Fuchs, B. M., Ludwig, W., Peplies, J., & Glöckner, F. O. (2007). SILVA: a comprehensive online resource for quality checked and aligned ribosomal RNA sequence data compatible with ARB. *Nucleic Acids Research, 35*(21), 7188-7196.

Puente and Bashan (1994), The desert epiphyte *Tillandsia recurvata* harbours the nitrogen-fixing bacterium *Pseudomonas stutzeri*, *Can J Bot*, *72*, 406-408

Qualls, R. G., & Haines, B. L. (1992). Biodegradability of dissolved organic matter in forest throughfall, soil solution, and stream water. *Soil Science Society of America Journal*, *56*(2), 578-586.

Qualls, R. G., Haines, B. L., & Swank, W. T. (1991). Fluxes of dissolved organic nutrients and humic substances in a deciduous forest. Ecology, 72(1), 254-266.

Quast, C., Pruesse, E., Yilmaz, P., Gerken, J., Schweer, T., Yarza, P., ... & Glöckner, F. O. (2012). The SILVA ribosomal RNA gene database project: improved data processing and web-based tools. *Nucleic acids research, 41*(D1), D590-D596.

Redford, A. J., Bowers, R. M., Knight, R., Linhart, Y., & Fierer, N. (2010). The ecology of the phyllosphere: geographic and phylogenetic variability in the distribution of bacteria on tree leaves. *Environmental microbiology*, *12*(11), 2885-2893.

R Development Core Team (2008). R: A language and environment for statistical computing. R Foundation for Statistical Computing, Vienna, Austria. ISBN 3-900051-07-0, URL http://www.R-project.org.

Rodà, F., Avila, A., & Bonilla, D. (1990). Precipitation, throughfall, soil solution and streamwater chemistry in a holm-oak (Quercus ilex) forest. Journal of Hydrology, 116(1-4), 167-183.

Rosier, C. L., Van Stan, J. T., Moore, L. D., Schrom, J. O., Wu, T., Reichard, J. S., & Kan, J. (2015). Forest canopy structural controls over throughfall affect soil microbial community structure in an epiphyte-laden maritime oak stand. Ecohydrology, 8(8), 1459-1470.

Šantl-Temkiv, T., Finster, K., Dittmar, T., Hansen, B. M., Thyrhaug, R., Nielsen, N. W., & Karlson, U. G. (2013). Hailstones: a window into the microbial and chemical inventory of a storm cloud. *PloS one*, *8*(1), e53550.

Savoie, D. L., & Prospero, J. M. (1980). Water-soluble potassium, calcium, and magnesium in the aerosols over the tropical North Atlantic. *Journal of Geophysical Research: Oceans*, *85*(C1), 385-392.

Schlesinger, W. H., & Marks, P. L. (1977). Mineral cycling and the niche of Spanish moss, Tillandsia usneoides L. *American Journal of Botany*, 1254-1262.

Silva, I. C., & Okumura, T. (1996). Throughfall, Stemflow and Interception Loss in a Mixed White Oak Forest (Quer-cus serrata Thunb.). Journal of forest research, 1(3), 123-129.

Sridhar, K. R., Karamchand, K. S., & Bhat, R. (2006). Arboreal water-borne hyphomycetes on oak-leaf basket fern Drynaria quercifolia. SYDOWIA-HORN-, 58(2), 309.

Tarrant, R. F., Lu, K. C., Bollen, W. B., & Chen, C. S. (1968). Nutrient cycling by throughfall and stemflow precipitation in three coastal Oregon forest types.*US, For. Serv., Res. Pap. PNW;(United States)*.

Thurow, T. L., Blackburn, W. H., Warren, S. D., & Taylor Jr, C. A. (1987). Rainfall interception by midgrass, shortgrass, and live oak mottes. *Journal of Range management*, 455-460.

Tukey Jr, H. B. (1970). The leaching of substances from plants. Annual review of plant physiology, 21(1), 305-324.

Twilley, R. R. (1985). The exchange of organic carbon in basin mangrove forests in a southwest Florida estuary. Estuarine, Coastal and shelf science, 20(5), 543-557.

Van Stan, John T., et al. "The effects of phenoseason and storm characteristics on throughfall solute washoff and leaching dynamics from a temperate deciduous forest canopy." *Science of the Total Environment* 430 (2012): 48-58.

Van Stan, J. T., Stubbins, A., Bittar, T., Reichard, J. S., Wright, K. A., & Jenkins, R. B. (2015). Tillandsia usneoides (L.) L.(Spanish moss) water storage and leachate characteristics from two maritime oak forest settings.*Ecohydrology*, *8*(6), 988-1004.

Vorholt, J. A. (2012). Microbial life in the phyllosphere. *Nature Reviews Microbiology*, *10*(12), 828-840.

Wang, Q., Garrity, G. M., Tiedje, J. M., & Cole, J. R. (2007). Naive Bayesian classifier for rapid assignment of rRNA sequences into the new bacterial taxonomy. *Applied and environmental microbiology, 73*(16), 5261-5267.

Ward, N. L., Challacombe, J. F., Janssen, P. H., Henrissat, B., Coutinho, P. M., Wu, M., ... & Barabote, R. D. (2009). Three genomes from the phylum Acidobacteria provide insight into the lifestyles of these microorganisms in soils. Applied and environmental microbiology, 75(7), 2046-2056.

Wilkinson, S. C., and J. M. Anderson. "Spatial patterns of soil microbial communities in a Norway spruce (Picea abies) plantation." *Microbial Ecology*42.3 (2001): 248-255.

Xu, Z., Malmer, D., Langille, M. G., Way, S. F., & Knight, R. (2014). Which is more important for classifying microbial communities: Who's there or what they can do? *The ISME Journal, 8*(12), 2357-2359. doi:10.1038/ismej.2014.157

Yilmaz, P., Parfrey, L. W., Yarza, P., Gerken, J., Pruesse, E., Quast, C., ... & Glöckner, F. O. (2013). The SILVA and "all-species living tree project (LTP)" taxonomic frameworks. *Nucleic acids research, 42*(D1), D643-D648.

Zimmermann, A., Wilcke, W., & Elsenbeer, H. (2007). Spatial and temporal patterns of throughfall quantity and quality in a tropical montane forest in Ecuador. Journal of Hydrology, 343(1), 80-96.

APPENDIX A

Bacterial community results for all storms

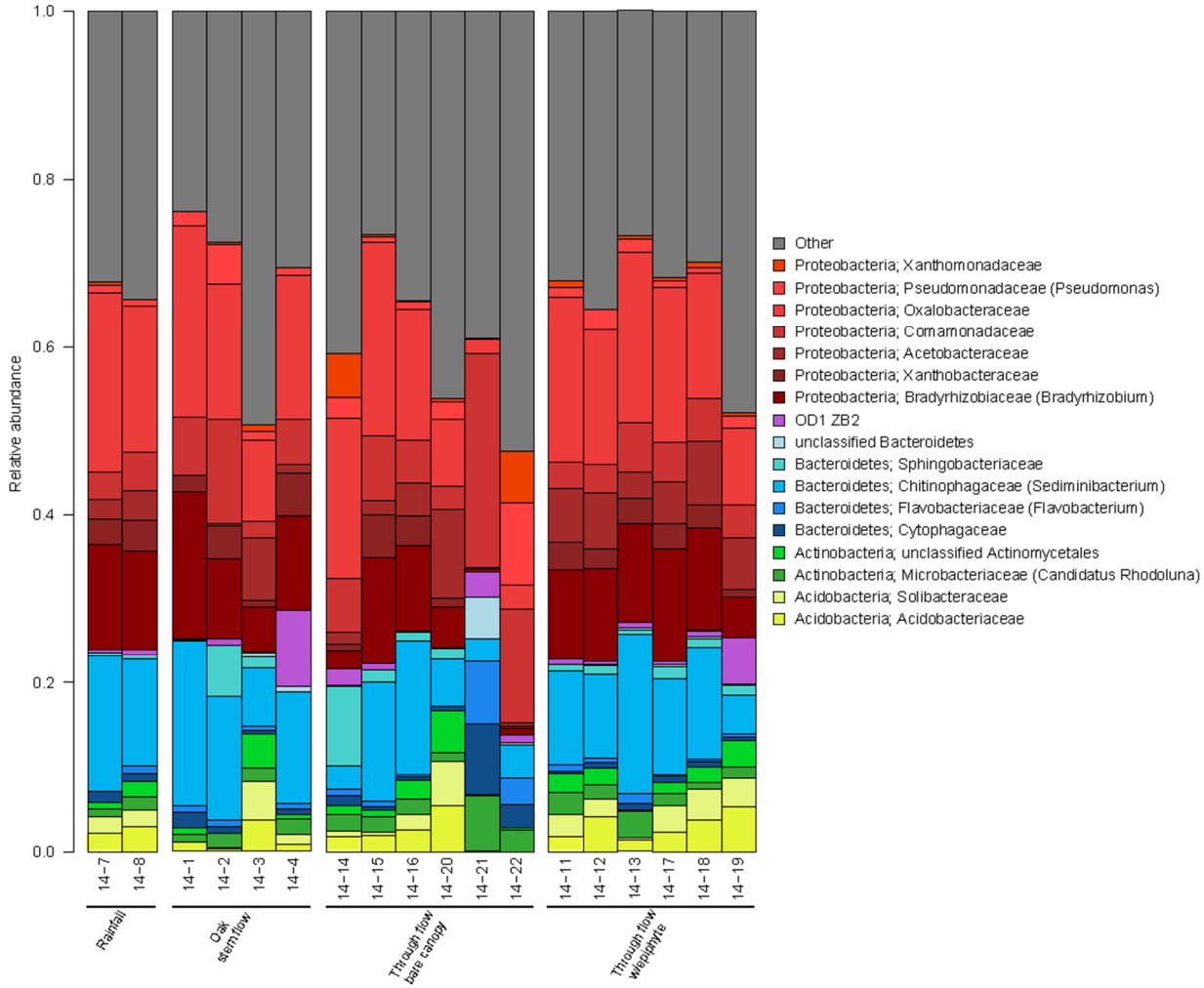

(Storm 14)

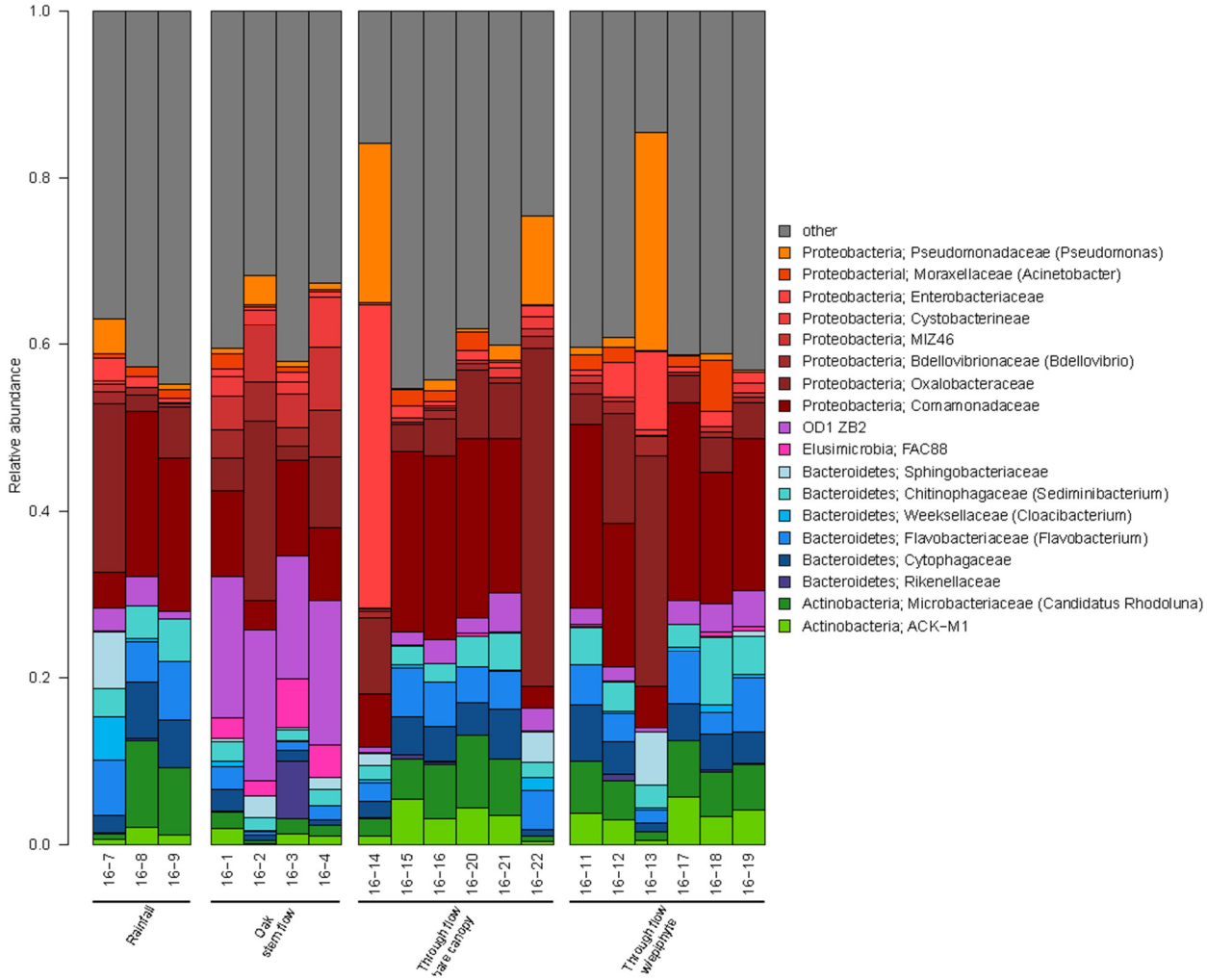
Relative abundance
1.0
0.8
0.6
0.4
0.2
0.0
16−7
16−8
16−9
16−1
16−2
16−3
16−4
16−14
16−15
16−16
16−20
16−21
16−22
16−11
16−12
16−13
16−17
16−18
16−19
Rainfall
Oak stemflow
Throughfall via canopy
Throughfall w/epiphyte
other
Proteobacteria; Pseudomonadaceae (Pseudomonas)
Proteobacterial; Moraxellaceae (Acinetobacter)
Proteobacteria; Enterobacteriaceae
Proteobacteria; Cystobacterineae
Proteobacteria; MIZ46
Proteobacteria; Bdellovibrionaceae (Bdellovibrio)
Proteobacteria; Oxalobacteraceae
Proteobacteria; Comamonadaceae
OD1 ZB2
Elusimicrobia; FAC88
Bacteroidetes; Sphingobacteriaceae
Bacteroidetes; Chitinophagaceae (Sediminibacterium)
Bacteroidetes; Weeksellaceae (Cloacibacterium)
Bacteroidetes; Flavobacteriaceae (Flavobacterium)
Bacteroidetes; Cytophagaceae
Bacteroidetes; Rikenellaceae
Actinobacteria; Microbacteriaceae (Candidatus Rhodoluna)
Actinobacteria; ACK−M1

(Storm 16)

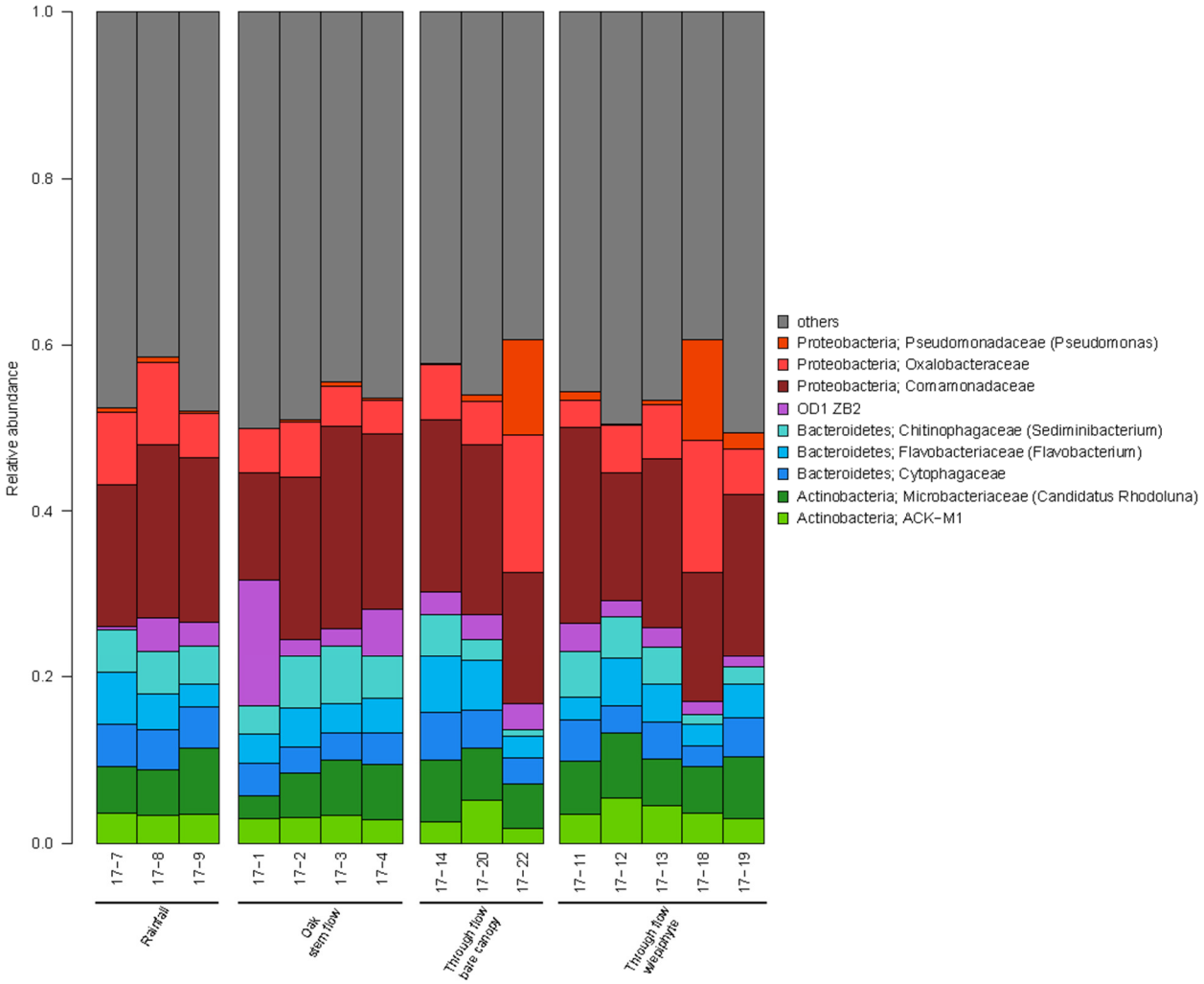
1.0
0.8
0.6
0.4
0.2
0.0
Relative abundance
others
Proteobacteria; Pseudomonadaceae (Pseudomonas)
Proteobacteria; Oxalobacteraceae
Proteobacteria; Comamonadaceae
OD1 ZB2
Bacteroidetes; Chitinophagaceae (Sediminibacterium)
Bacteroidetes; Flavobacteriaceae (Flavobacterium)
Bacteroidetes; Cytophagaceae
Actinobacteria; Microbacteriaceae (Candidatus Rhodoluna)
Actinobacteria; ACK-M1
17-7
17-8
17-9
17-1
17-2
17-3
17-4
17-14
17-20
17-22
17-11
17-12
17-13
17-18
17-19
Rainfall
Oak stem flow
Through flow bare canopy
Through flow epiphyte

(Storm 17)

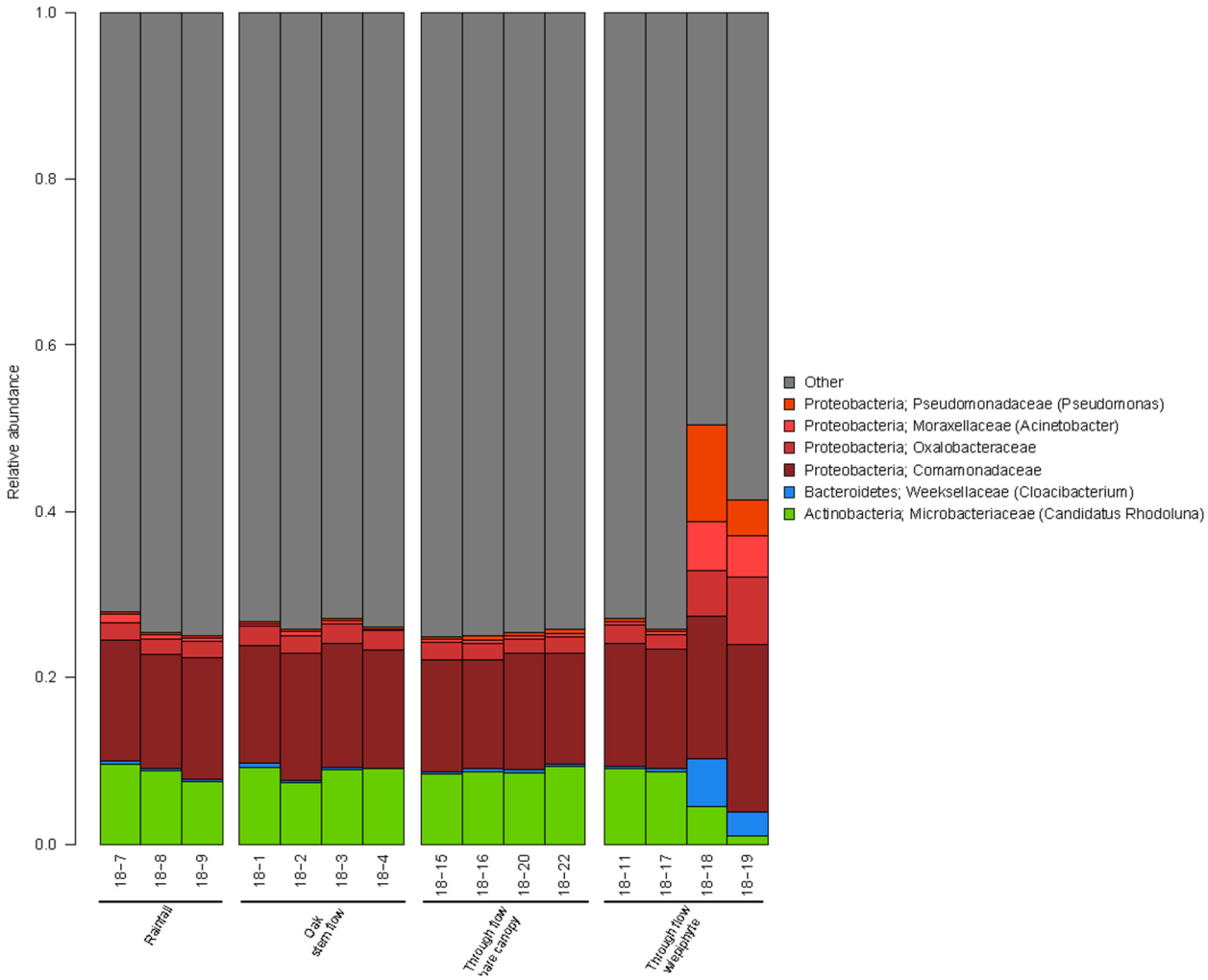
1.0
0.8
0.6
0.4
0.2
0.0
Relative abundance
Other
Proteobacteria; Pseudomonadaceae (Pseudomonas)
Proteobacteria; Moraxellaceae (Acinetobacter)
Proteobacteria; Oxalobacteraceae
Proteobacteria; Comamonadaceae
Bacteroidetes; Weeksellaceae (Cloacibacterium)
Actinobacteria; Microbacteriaceae (Candidatus Rhodoluna)
18-7
18-8
18-9
18-1
18-2
18-3
18-4
18-15
18-16
18-20
18-22
18-11
18-17
18-18
18-19
Rainfall
Oak stemflow
Throughfall vate canopy
Throughfall wiepiphyte

(Storm 18)

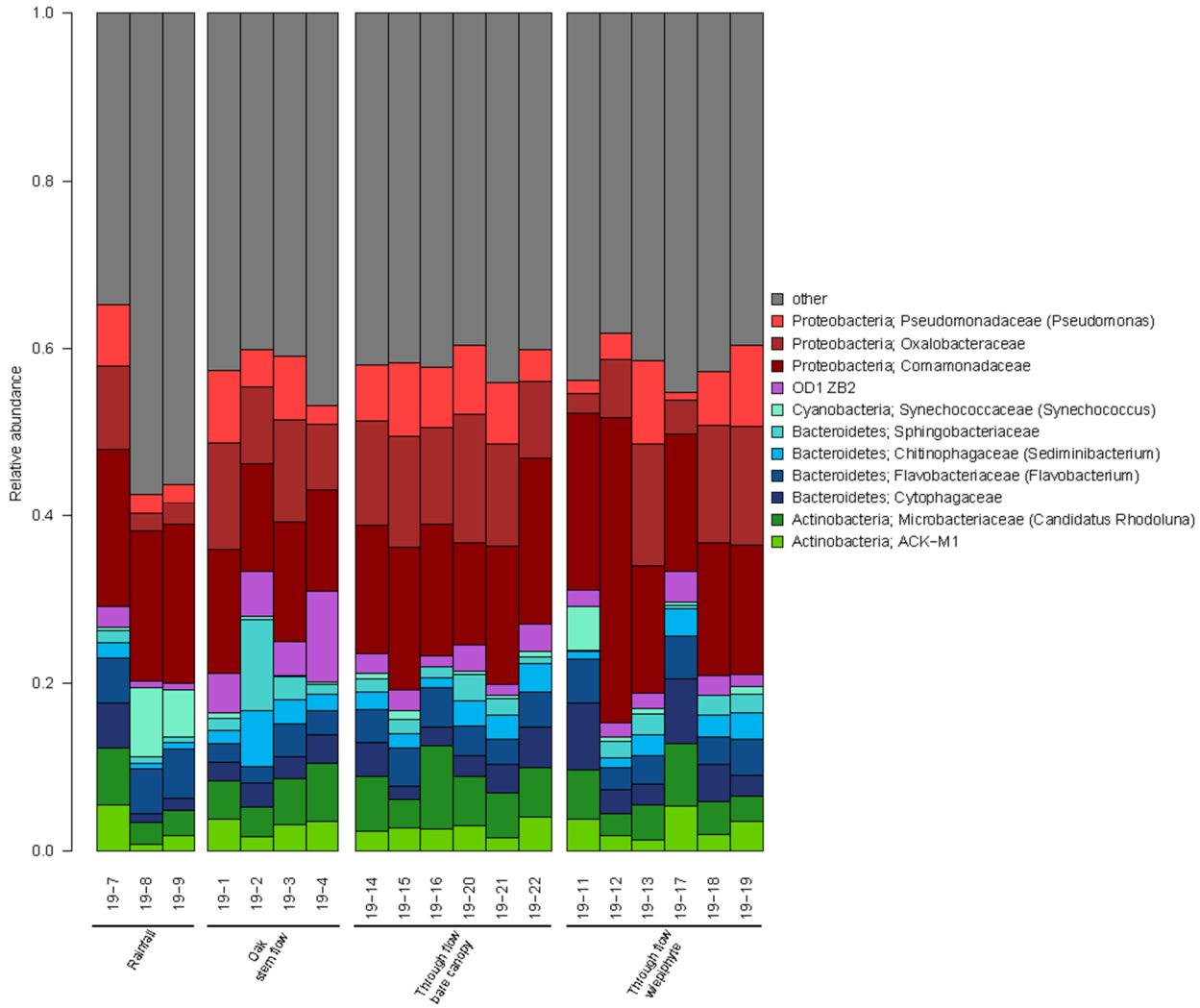
1.0
0.8
0.6
0.4
0.2
0.0
Relative abundance
other
Proteobacteria; Pseudomonadaceae (Pseudomonas)
Proteobacteria; Oxalobacteraceae
Proteobacteria; Comamonadaceae
OD1 ZB2
Cyanobacteria; Synechococcaceae (Synechococcus)
Bacteroidetes; Sphingobacteriaceae
Bacteroidetes; Chitinophagaceae (Sediminibacterium)
Bacteroidetes; Flavobacteriaceae (Flavobacterium)
Bacteroidetes; Cytophagaceae
Actinobacteria; Microbacteriaceae (Candidatus Rhodoluna)
Actinobacteria; ACK-M1
19-7
19-8
19-9
19-1
19-2
19-3
19-4
19-14
19-15
19-16
19-20
19-21
19-22
19-11
19-12
19-13
19-17
19-18
19-19
Rainfall
Oak stem flow
Through flow bare canopy
Through flow epiphyte

(Storm 19)

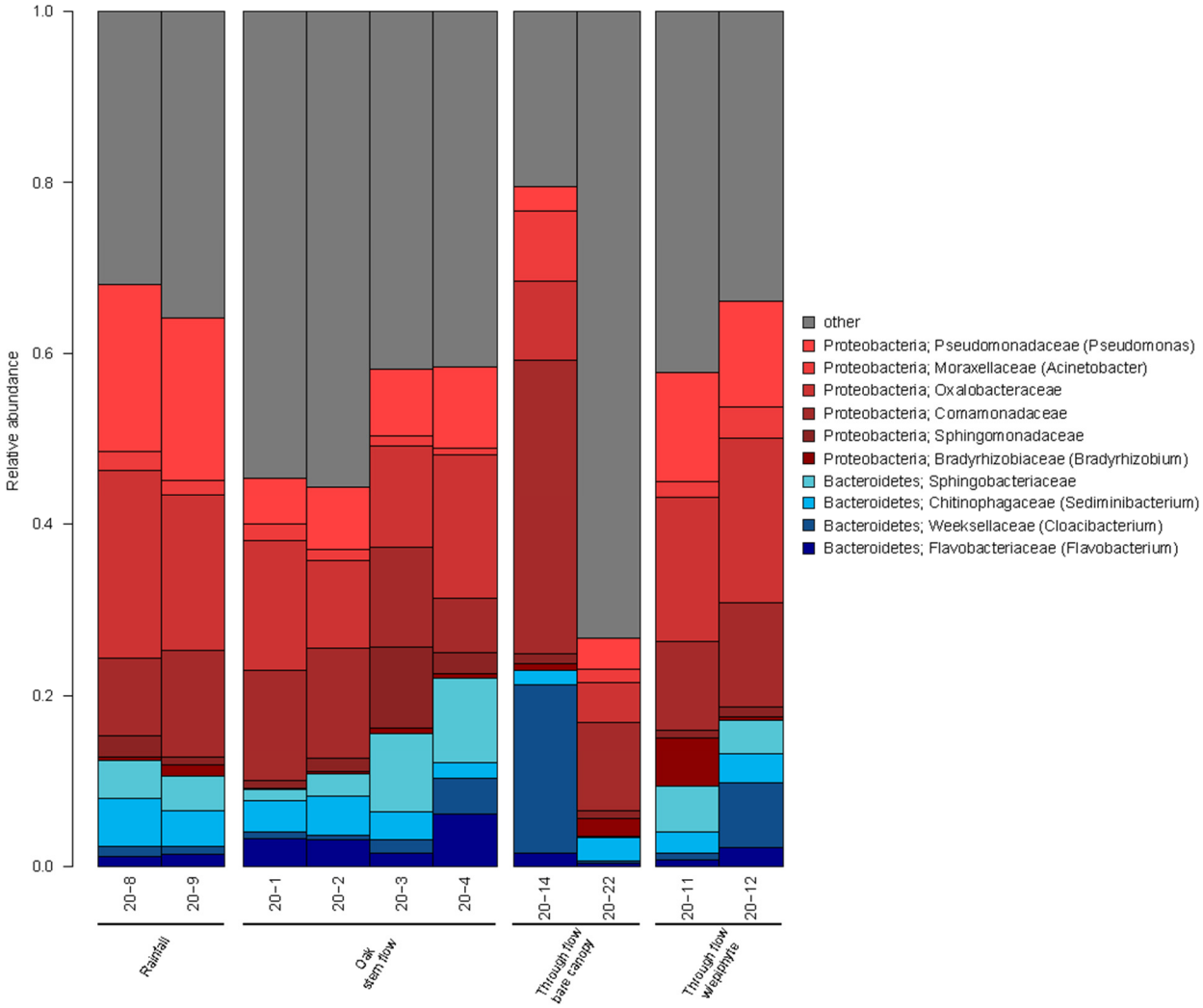
Relative abundance
1.0
0.8
0.6
0.4
0.2
0.0
20-8
20-9
20-1
20-2
20-3
20-4
20-14
20-22
20-11
20-12
Rainfall
Oak stem flow
Through flow bare canopy
Through flow epiphyte
other
Proteobacteria; Pseudomonadaceae (Pseudomonas)
Proteobacteria; Moraxellaceae (Acinetobacter)
Proteobacteria; Oxalobacteraceae
Proteobacteria; Comamonadaceae
Proteobacteria; Sphingomonadaceae
Proteobacteria; Bradyrhizobiaceae (Bradyrhizobium)
Bacteroidetes; Sphingobacteriaceae
Bacteroidetes; Chitinophagaceae (Sediminibacterium)
Bacteroidetes; Weeksellaceae (Cloacibacterium)
Bacteroidetes; Flavobacteriaceae (Flavobacterium)

(Storm 20)

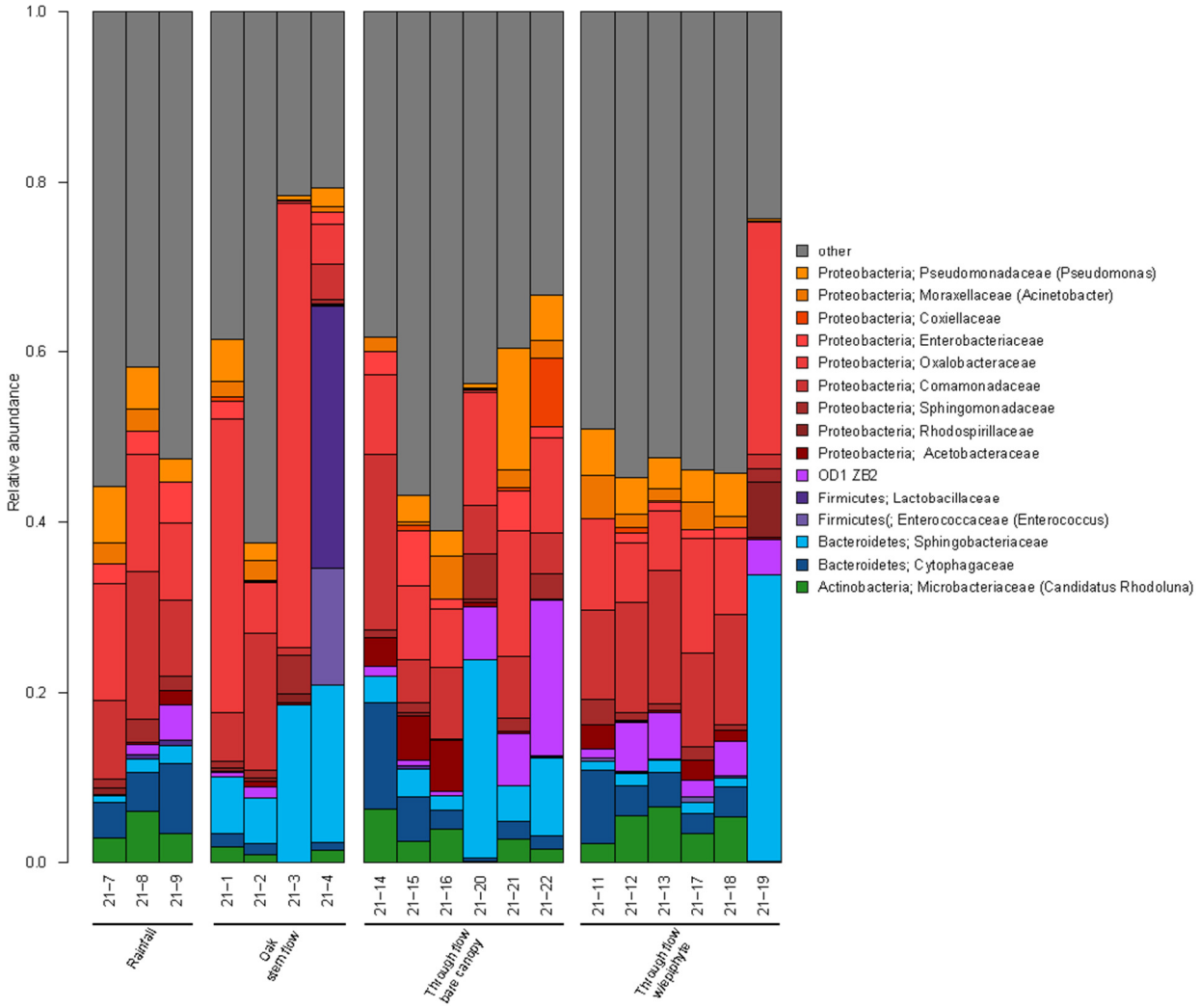
1.0
0.8
0.6
0.4
0.2
0.0
Relative abundance
21–7
21–8
21–9
21–1
21–2
21–3
21–4
21–14
21–15
21–16
21–20
21–21
21–22
21–11
21–12
21–13
21–17
21–18
21–19
Rainfall
Oak stem flow
Through flow bare canopy
Through flow epiphyte
other
Proteobacteria; Pseudomonadaceae (Pseudomonas)
Proteobacteria; Moraxellaceae (Acinetobacter)
Proteobacteria; Coxiellaceae
Proteobacteria; Enterobacteriaceae
Proteobacteria; Oxalobacteraceae
Proteobacteria; Comamonadaceae
Proteobacteria; Sphingomonadaceae
Proteobacteria; Rhodospirillaceae
Proteobacteria; Acetobacteraceae
OD1 ZB2
Firmicutes; Lactobacillaceae
Firmicutes(; Enterococcaceae (Enterococcus)
Bacteroidetes; Sphingobacteriaceae
Bacteroidetes; Cytophagaceae
Actinobacteria; Microbacteriaceae (Candidatus Rhodoluna)

(Storm 21)

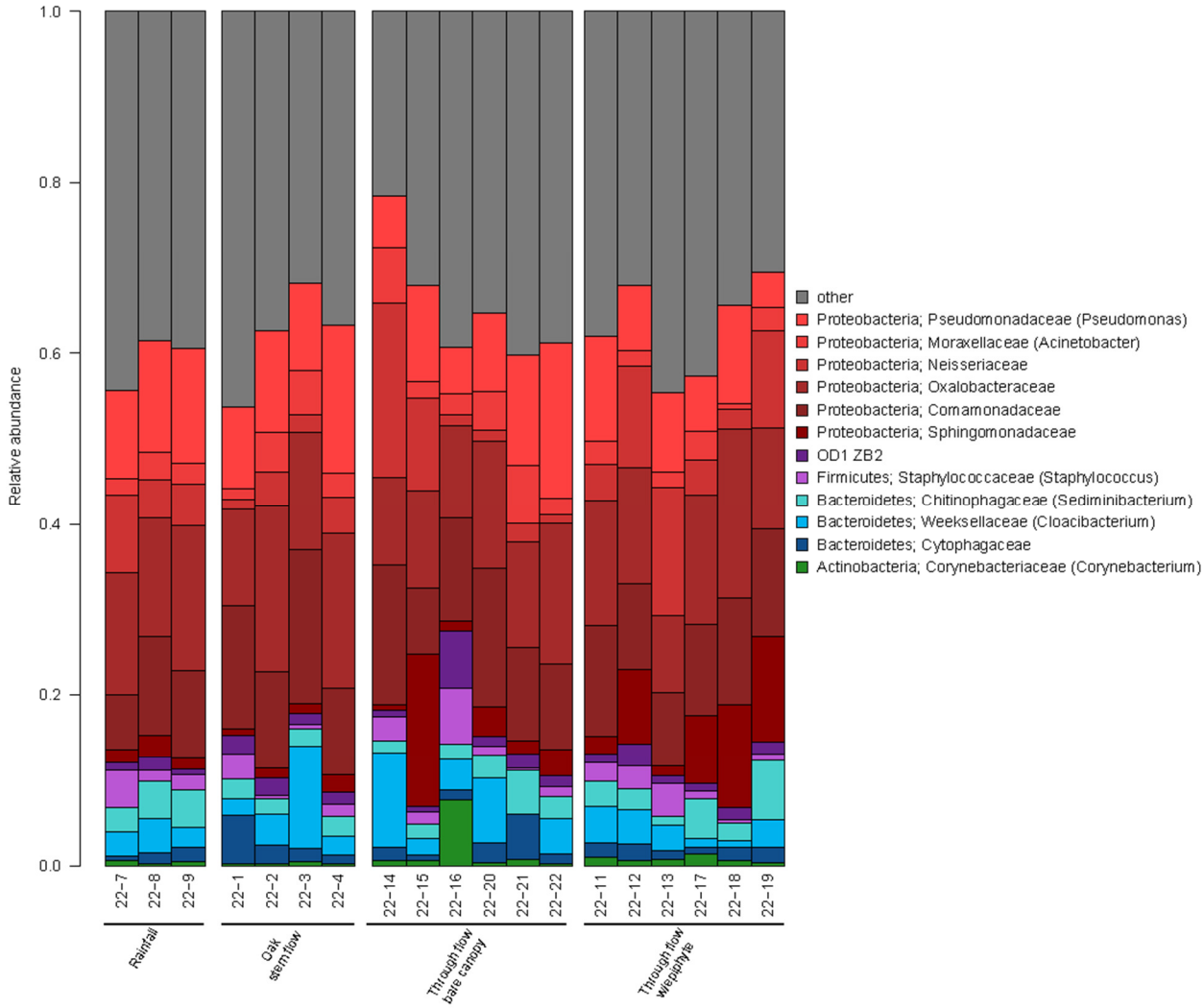
Relative abundance
1.0
0.8
0.6
0.4
0.2
0.0
22−7
22−8
22−9
22−1
22−2
22−3
22−4
22−14
22−15
22−16
22−20
22−21
22−22
22−11
22−12
22−13
22−17
22−18
22−19
Rainfall
Oak stemflow
Throughfow bare canopy
Throughfow wiregrass
other
Proteobacteria; Pseudomonadaceae (Pseudomonas)
Proteobacteria; Moraxellaceae (Acinetobacter)
Proteobacteria; Neisseriaceae
Proteobacteria; Oxalobacteraceae
Proteobacteria; Comamonadaceae
Proteobacteria; Sphingomonadaceae
OD1 ZB2
Firmicutes; Staphylococcaceae (Staphylococcus)
Bacteroidetes; Chitinophagaceae (Sediminibacterium)
Bacteroidetes; Weeksellaceae (Cloacibacterium)
Bacteroidetes; Cytophagaceae
Actinobacteria; Corynebacteriaceae (Corynebacterium)

(Storm 22)

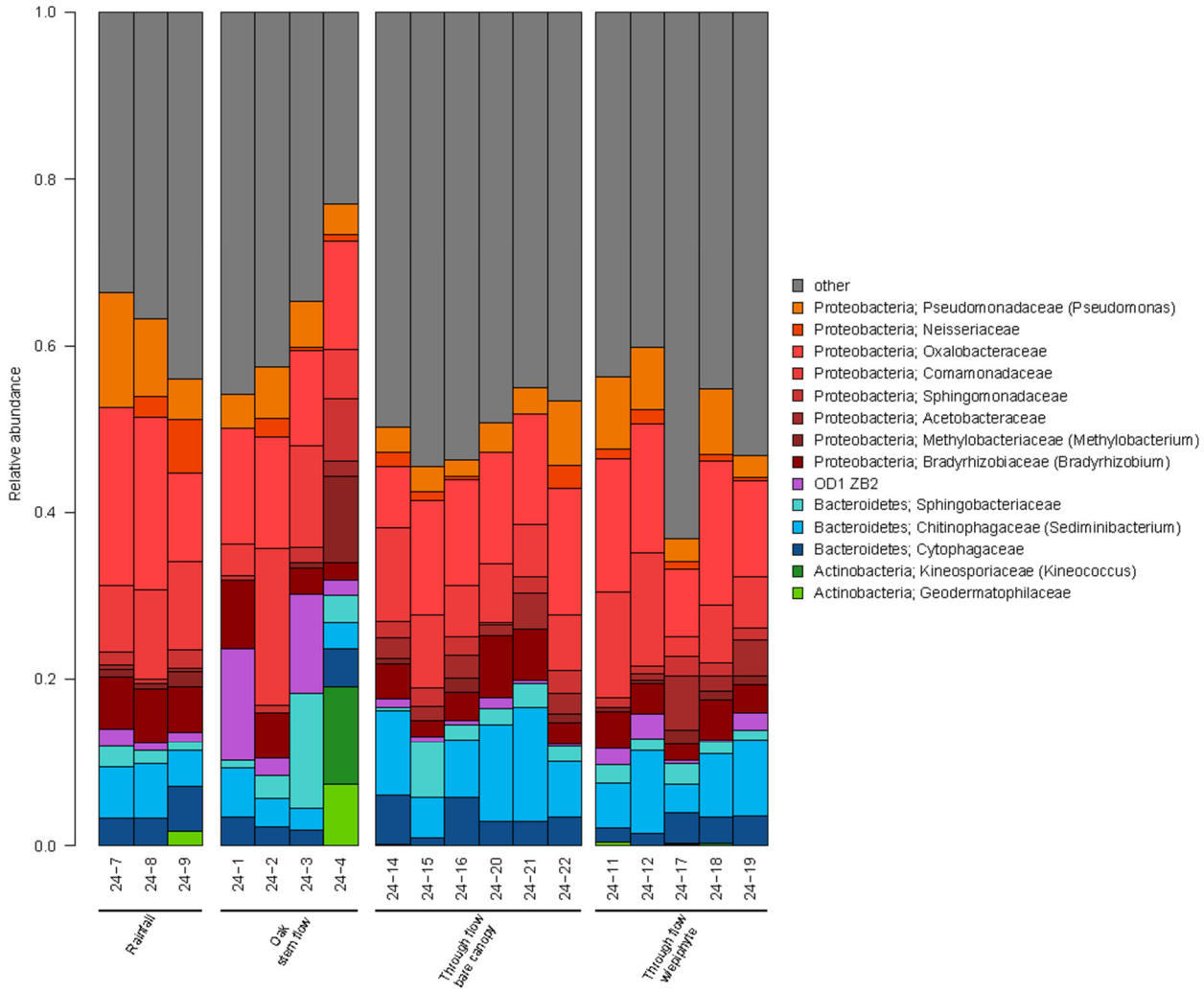
1.0
0.8
0.6
0.4
0.2
0.0
Relative abundance
24-7
24-8
24-9
24-1
24-2
24-3
24-4
24-14
24-15
24-16
24-20
24-21
24-22
24-11
24-12
24-17
24-18
24-19
Rainfall
Oak stem flow
Through flow bare canopy
Through flow epiphyte
other
Proteobacteria; Pseudomonadaceae (Pseudomonas)
Proteobacteria; Neisseriaceae
Proteobacteria; Oxalobacteraceae
Proteobacteria; Comamonadaceae
Proteobacteria; Sphingomonadaceae
Proteobacteria; Acetobacteraceae
Proteobacteria; Methylobacteriaceae (Methylobacterium)
Proteobacteria; Bradyrhizobiaceae (Bradyrhizobium)
OD1 ZB2
Bacteroidetes; Sphingobacteriaceae
Bacteroidetes; Chitinophagaceae (Sediminibacterium)
Bacteroidetes; Cytophagaceae
Actinobacteria; Kineosporiaceae (Kineococcus)
Actinobacteria; Geodermatophilaceae

(Storm 24)

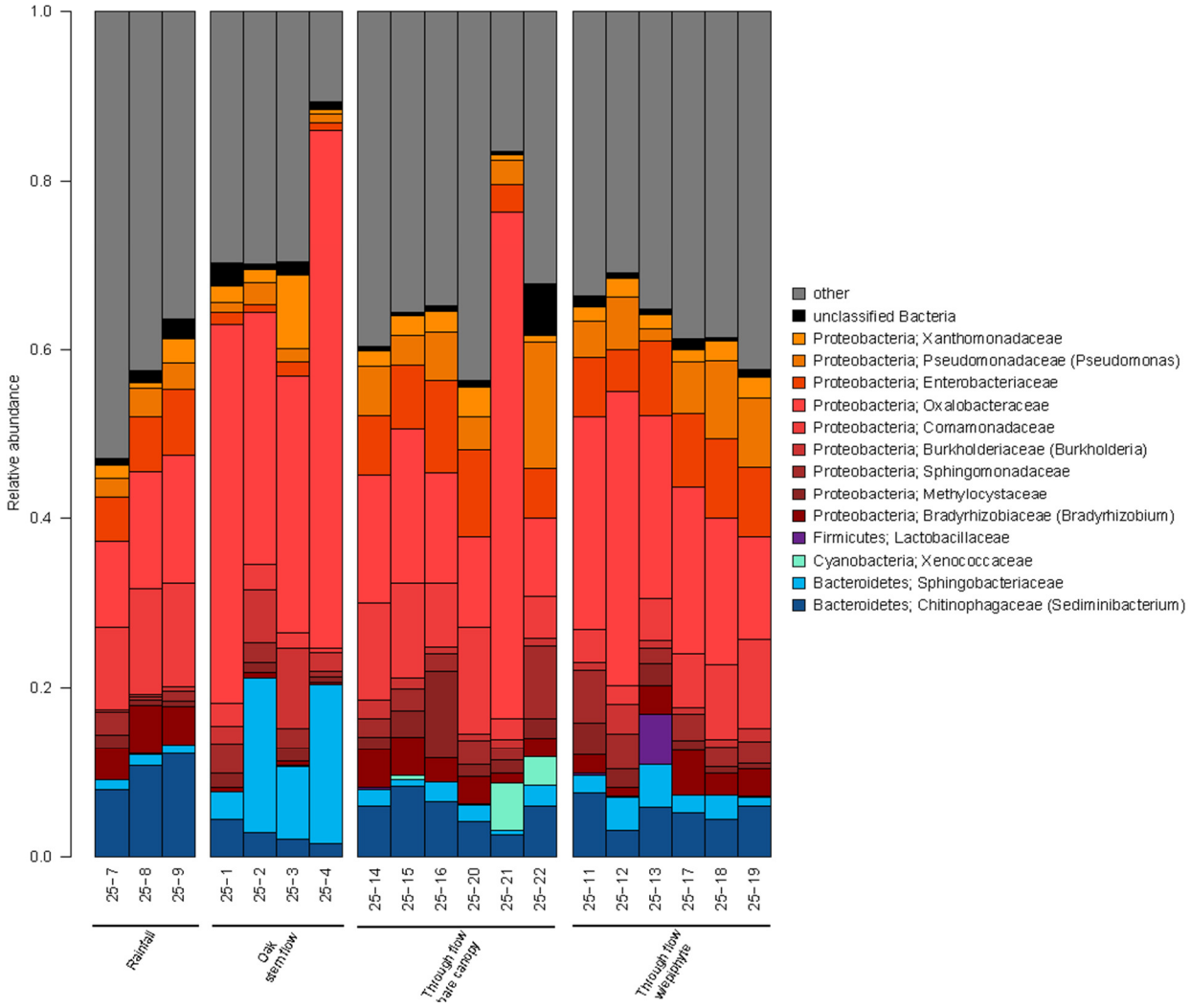
Relative abundance
1.0
0.8
0.6
0.4
0.2
0.0
25−7
25−8
25−9
25−1
25−2
25−3
25−4
25−14
25−15
25−16
25−20
25−21
25−22
25−11
25−12
25−13
25−17
25−18
25−19
Rainfall
Oak stemflow
Through flow
Through flow
other
unclassified Bacteria
Proteobacteria; Xanthomonadaceae
Proteobacteria; Pseudomonadaceae (Pseudomonas)
Proteobacteria; Enterobacteriaceae
Proteobacteria; Oxalobacteraceae
Proteobacteria; Comamonadaceae
Proteobacteria; Burkholderiaceae (Burkholderia)
Proteobacteria; Sphingomonadaceae
Proteobacteria; Methylocystaceae
Proteobacteria; Bradyrhizobiaceae (Bradyrhizobium)
Firmicutes; Lactobacillaceae
Cyanobacteria; Xenococcaceae
Bacteroidetes; Sphingobacteriaceae
Bacteroidetes; Chitinophagaceae (Sediminibacterium)

(Storm 25)

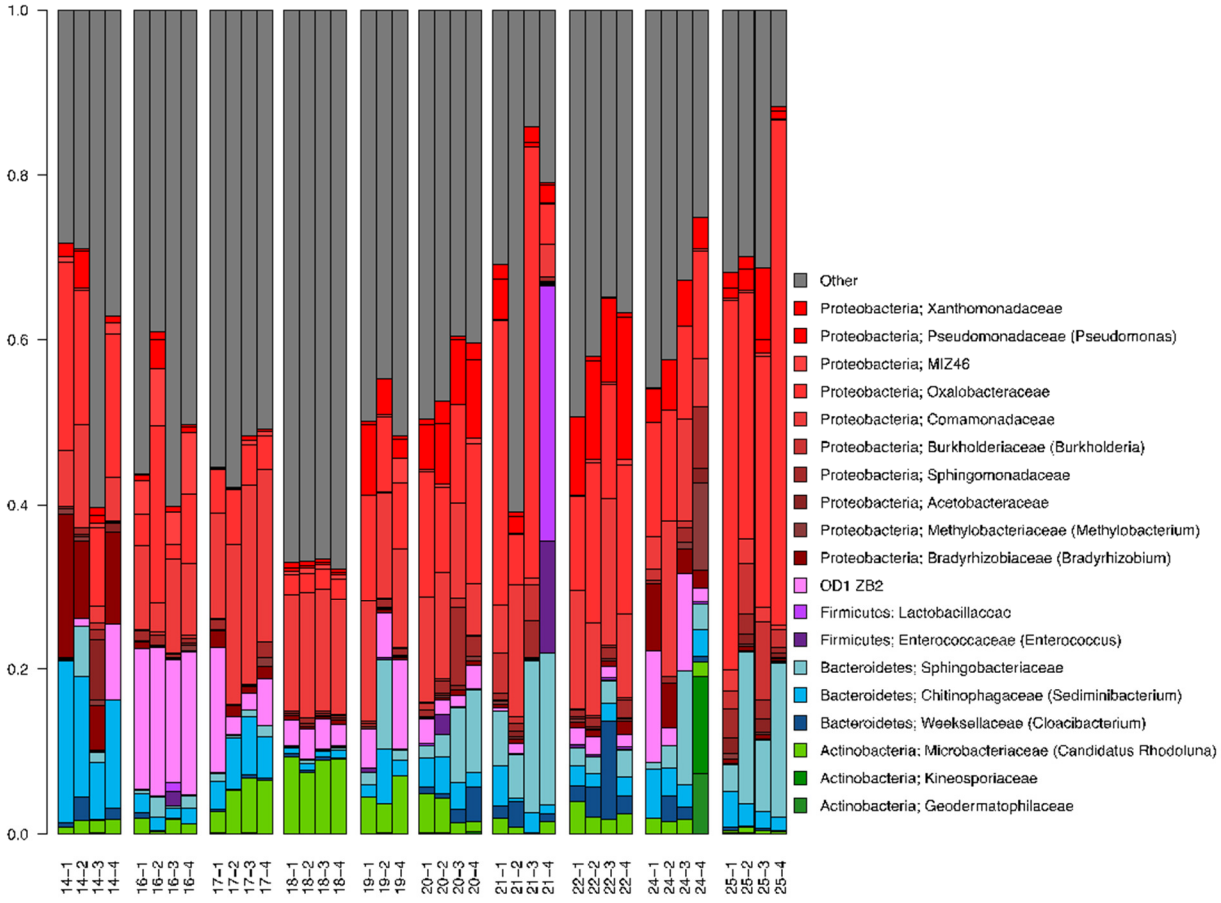

(All SF Samples)

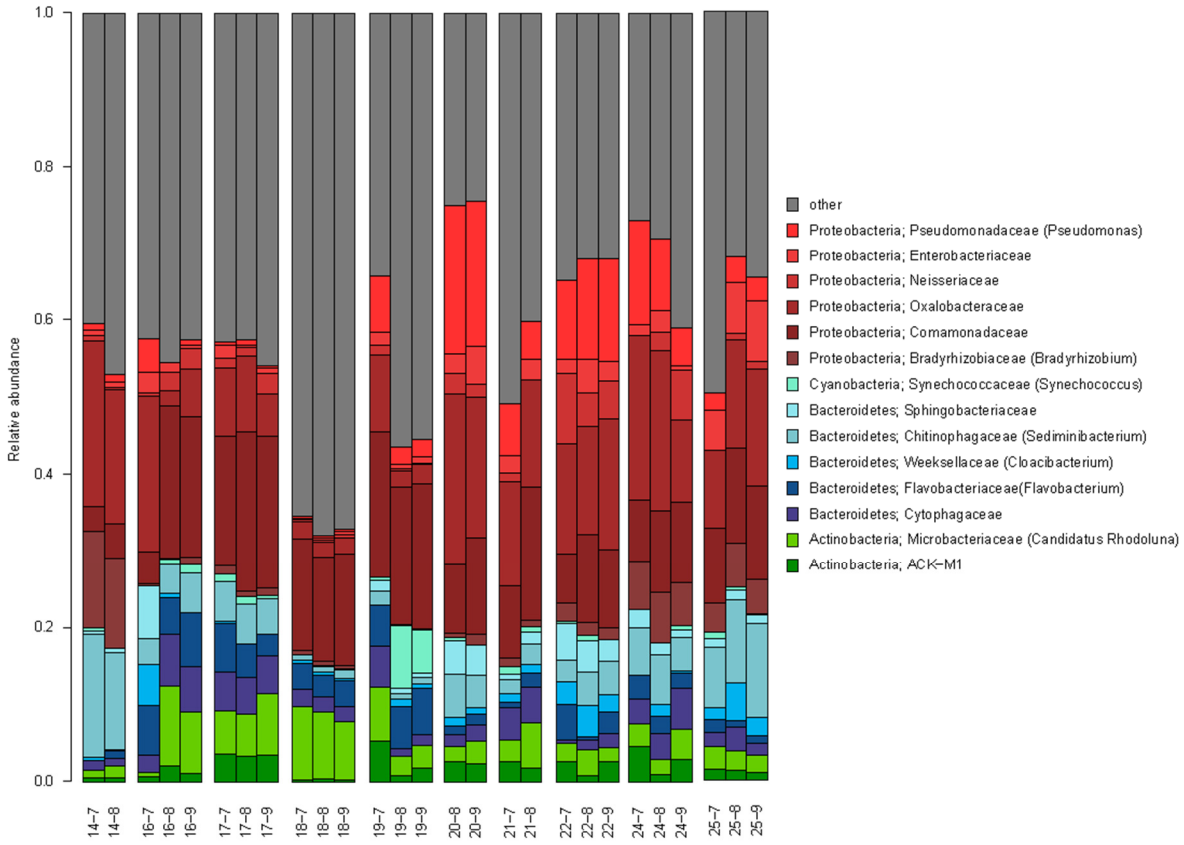

(All Rain Samples)

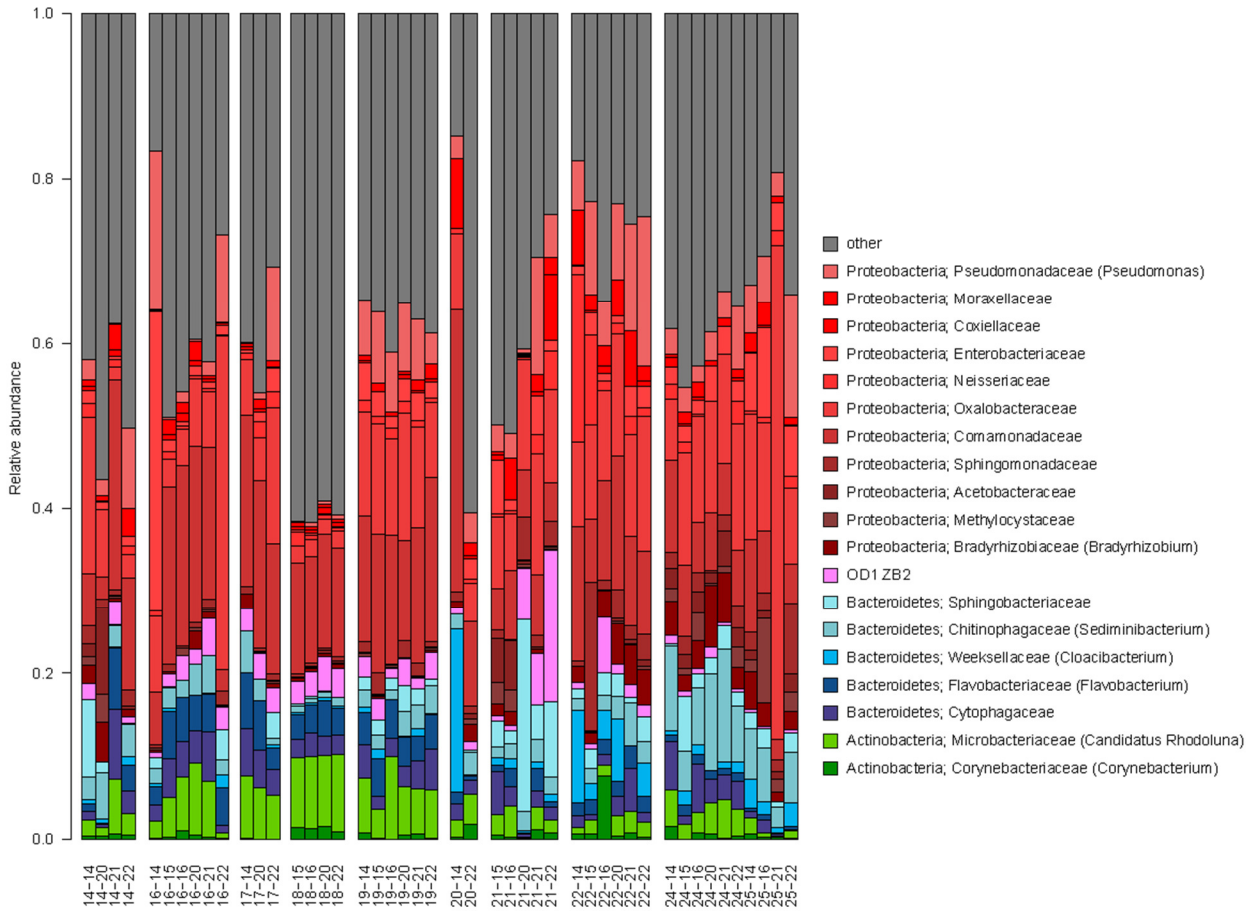

(Bare TF Samples)

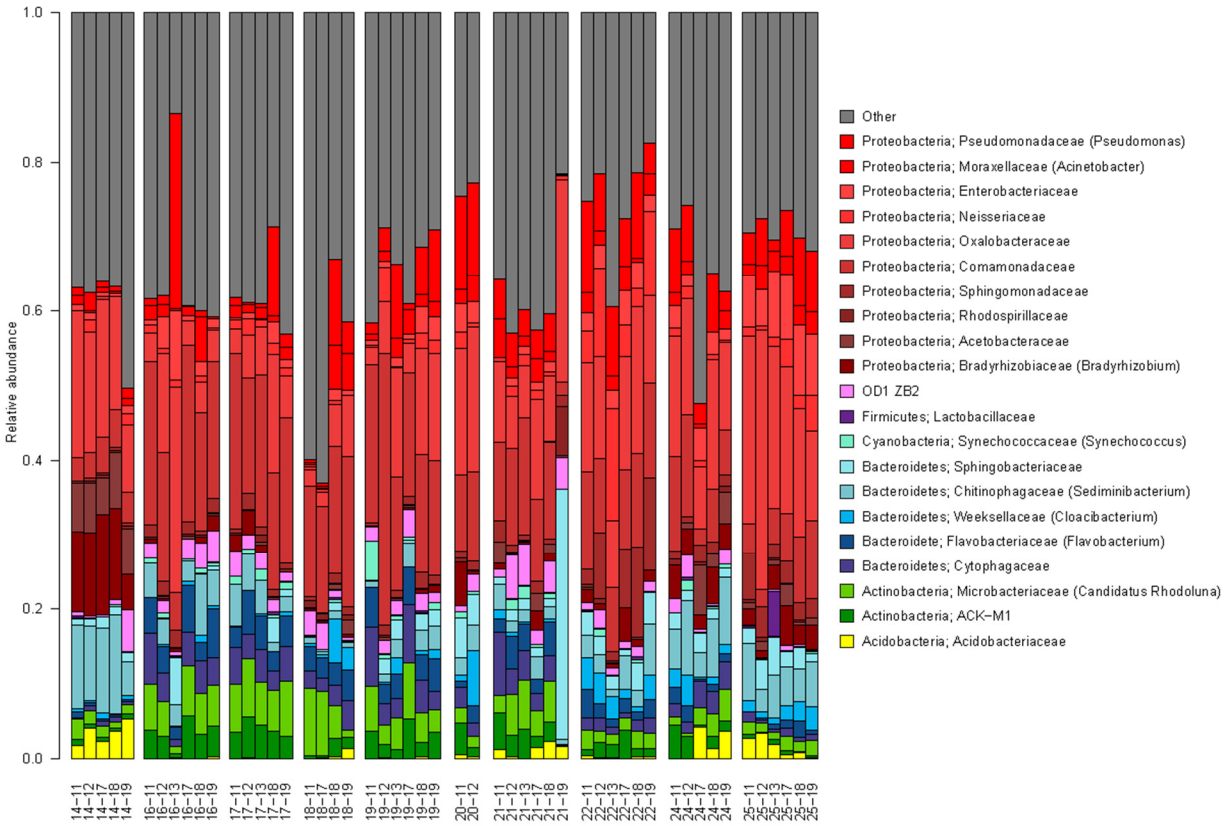

(Epiphyte Covered TF Samples)